

The quest for new correlations in the realm of the Gamma-Ray Burst - Supernova connection

M. G. DAINOTTI ,^{1,2,3} B. DE SIMONE ,^{4,5} M. I. KHADIR ,⁶ K. KAWAGUCHI ,⁷ T. J. MORIYA ,^{1,2,8}
 T. TAKIWAKI ,^{1,2} N. TOMINAGA ,^{1,2,9,10} AND A. GANGOPADHYAY ,¹¹

¹National Astronomical Observatory of Japan, 2 Chome-21-1 Osawa, Mitaka, Tokyo 181-8588, Japan

²The Graduate University for Advanced Studies, SOKENDAI, Shonanokusaimura, Hayama, Miura District, Kanagawa 240-0193, Japan

³Space Science Institute, Boulder, CO, USA

⁴Department of Physics "E. R. Caianiello" - Università degli Studi di Salerno - Via Giovanni Paolo II, 132, 84084 Fisciano SA

⁵INFN Gruppo Collegato di Salerno - Sezione di Napoli - Via Giovanni Paolo II, 132, 84084 Fisciano SA

⁶Department of Physics, University of Constantine 1 - RN79, Constantine, Algeria

⁷Faculty of Science, Kumamoto University, 2-39-1 Kurokami, Chuo Ward, Kumamoto, Kumamoto Prefecture 860-0862, Japan

⁸School of Physics and Astronomy, Faculty of Science, Monash University, Clayton, Victoria 3800, Australia

⁹Kavli Institute for the Physics and Mathematics of the Universe (WPI), The University of Tokyo Institutes for Advanced Study, The University of Tokyo, 5-1-5 Kashiwanoha, Kashiwa, Chiba 277-8583, Japan

¹⁰Department of Physics, Faculty of Science and Engineering, Konan University, 8-9-1 Okamoto, Kobe, Hyogo 658-8501, Japan

¹¹Hiroshima Astrophysical Science Center, Hiroshima University, Higashi-Hiroshima, Japan

ABSTRACT

Gamma-Ray Bursts (GRBs) are very energetic cosmological transients. Long GRBs are usually associated with Type Ib/c Supernovae (SNe), and we refer to them as GRB-SNe. Since the associated SN for a given GRB is observed only at low redshift, a possible selection effect exists when we consider intrinsically faint sources which cannot be observed at high redshift. Thus, it is important to explore the possible relationships between GRB and SN parameters after these have been corrected for astrophysical biases due to the instrumental selection effects and redshift evolution of the variables involved. So far, only GRB prompt emission properties have been checked against the SNe Ib/c properties without considering the afterglow (AG). This work investigates the existence of relationships among GRB's prompt and AG and associated SN properties. We investigate 91 bidimensional correlations among the SN and GRB observables before and after their correction for selection biases and evolutionary effects. As a result of this investigation, we find hints of a new correlation with a Pearson correlation coefficient > 0.50 and a probability of being drawn by chance < 0.05 . This correlation is between the luminosity at the end of the GRB optical plateau emission and the rest-frame peak time of the SN. According to this relation, the brightest optical plateaus are accompanied by the largest peak times. This correlation is corrected for selection biases and redshift evolution and may provide new constraints for the astrophysical models associated with the GRB-SNe connection.

Keywords: Gamma-ray bursts (629) — Core-collapse supernovae (304)

1. INTRODUCTION

Gamma-ray Bursts (GRBs) are bright and short γ -ray flashes. During their short durations, they emit the same energy that the Sun will have released at the end of its life starting from its birth: their isotropic energy ranges from 10^{47} to 10^{54} erg.

Mazets et al. (1981) and Kouveliotou et al. (1993) discovered a bimodality distribution of the duration of GRBs prompt emission in their observer frame with the analysis of the first BATSE catalog. Based on their findings, they defined two classes of GRBs: Short (SGRBs, with the prompt duration, T_{90} ¹ shorter than 2 seconds) and Long (LGRBs, with $T_{90} > 2$ seconds). This bi-modality was proven to hold also in the rest-frame. SGRBs originate from binary mergers: the merging of a binary neutron star (NS) or an NS with a black hole (BH). The binary NS merger has

¹ It is the time during which a GRB emits 90% of its energy (from 5% to 95%).

given rise to the GW observed in association with the SGRB 170817A (Abbott et al. 2017; Pian et al. 2017; Troja et al. 2017). Instead, traditionally the LGRBs are thought to be generated from the Core-Collapse (CC) of massive stars, the Wolf-Rayet (W-R, Biermann & Cassinelli 1993; Usov 1994; Schaefer et al. 1994). For a later discussion on this classification based on the observations of the Neil Gehrels Swift Observatory (hereafter Swift satellite, 2004-ongoing) GRBs, one can refer to Bromberg et al. (2013).

Among all the phenomenological classes of GRBs, an interesting role is played by the GRBs associated with Type Ib or Ic Supernovae (SNe Ib/Ic). We here refer to these associations as GRB-SNe (Wang & Wheeler 1998; Ruffini et al. 2001; Woosley & Bloom 2006; Nomoto et al. 2010; Hjorth 2013; Cano 2011; Rueda & Ruffini 2012; Cano 2014; Cano et al. 2017a; Guessoum et al. 2017; Aguilera-Dena et al. 2018; Gompertz et al. 2020; Moriya et al. 2020), which are studied here. We here recall that most of the nearby LGRBs are believed to be associated with an SN, but only a fraction of them (2-7%) are visible due to instrumental selection biases (Rossi et al. 2021). On the other hand, a fraction of SNe Ib/c smaller than $\sim 10\%$ is associated with a GRB (Soderberg et al. 2006a). An estimation of the ratio between GRBs and SNe Ib/Ic leads to a percentage of GRB/SNe $\sim 1 - 9\%$ (Guetta & Valle 2007; Ruffini et al. 2016).

The debate of whether or not all the LGRBs are associated with SNe has been fomented for a long time since 2006. Indeed, Della Valle et al. 2006; Fynbo et al. 2006; Melandri et al. 2014 discussed cases of GRBs for which the SNe should have been seen if these were associated with the underlined GRBs: in particular, these are the cases of GRB 060614 and 060505. The first GRB has also revealed a Short with Extended Emission nature (Kaneko et al. 2015), while for the latter the SN associated has been debated by various authors (Ofek et al. 2007).

In the GRB-SNe events, the connection is often established by looking at the late times of their optical light curves (LCs) where the associated SNe usually show a photometric feature that points out their presence, namely a bump in the LC (Cano 2011). Usually, for a GRB-SN associated event, in the late time of the optical LC three main components emerge: (I) the GRB AG, (II) the contribution from the host galaxy, and (III) the SN identified through the bump.

Concerning the morphology of GRBs, their LCs show two main phases: the prompt emission, where we observe the main event in γ -rays and hard X-rays, and the subsequent afterglow (AG), which is observed in soft X-rays, optical, and sometimes in radio.

The launch of the Swift satellite (Gehrels 2004; Sakamoto et al. 2008) has uncovered a more peculiar behavior of the GRB LC than the simple power-law trend, this latter being explained within the traditional fireball model (Granot et al. 1999; Piran 1999; Meszaros 2000; Piran 2000; Mészáros 2001; Granot & Sari 2002). More specifically, the Swift satellite has discovered the existence of a new exciting feature in the AG phase: the plateau emission. This flattening, which happens after the abrupt luminosity decrease of the prompt emission, is observed for more than 42% of Swift X-ray LGRBs (Evans et al. 2009), see the upper panel of Figure 1. Not only is the prompt emission at the center of the investigation for the search for relevant correlations, but also the plateau emission has been studied for this purpose.

The search in the AG properties is crucial as a step forward to building a standard candle. The plateau emission properties are appealing for the search for new correlations because the plateau features are more regular (e.g. they have no variability as is shown in the prompt emission) than the prompt ones. Indeed, once the prompt is available, the plateau emission, if present, is visible thanks to the Swift satellite XRT instrument.

The plateau emission is involved in many relevant correlations between prompt and AG parameters in the GRB emission. We here mention the correlation between the X-ray end time of the plateau emission in the rest-frame ($\log T_{a,X}^*$) and its correspondent luminosity in the same band ($\log L_{a,X}$), the so-called Dainotti relation (Dainotti et al. 2008, 2013, 2015; Dainotti & Del Vecchio 2017). This correlation means that the more luminous the plateau emission, the shorter its duration. Since the slope of this correlation is -1, this means that the energy reservoir of the plateau is constant. There are also the prompt-AG relations between $L_{a,X}$ and the 1-second X-ray peak luminosity of the GRB (L_{peak}), see Dainotti et al. (2011, 2015). The former has been recently discovered also in the optical wavelengths (Dainotti et al. 2020b). Extending the 2-dimensional relation into a 3-dimensional relation adding the L_{peak} to $L_{a,X}$ and $T_{a,X}^*$, a 3-dimensional relation can be found, called the fundamental plane relation (Dainotti et al. 2016, 2017a,b, 2020a; Cao et al. 2022a,b).

Many GRB correlations regarding the prompt emission have been discovered during the last 20 years: the Amati relation (Amati et al. 2002; Ghisellini et al. 2006; Campana et al. 2007; Amati 2008; Martone et al. 2017), the Yonetoku relation (Yonetoku et al. 2004; Ito et al. 2019), the Ghirlanda relation (Liang & Zhang 2005; Ghirlanda et al. 2004; Ghirlanda et al. 2010), the correlation between the intrinsic brightness and the decay rate of Swift GRBs detected with the UVOT instrument (Oates et al. 2012), the Tsutsui relation (Tsutsui et al. 2013; Tsutsui & Shigeyama 2013).

However, a discussion on the prompt relations concerning the GRB prompt variables and their selection biases have been discussed in (Shahmoradi & Nemiroff 2015). Among these, the Amati, the Ghirlanda, and the Tsutsui relations hold also for the case of GRB-SNe, while for the AG relations we here mention that the 2-dimensional Dainotti relations in X-rays and in optical (Dainotti et al. 2008, 2013, 2015, 2020b) are fulfilled also for the GRB-SNe cases.

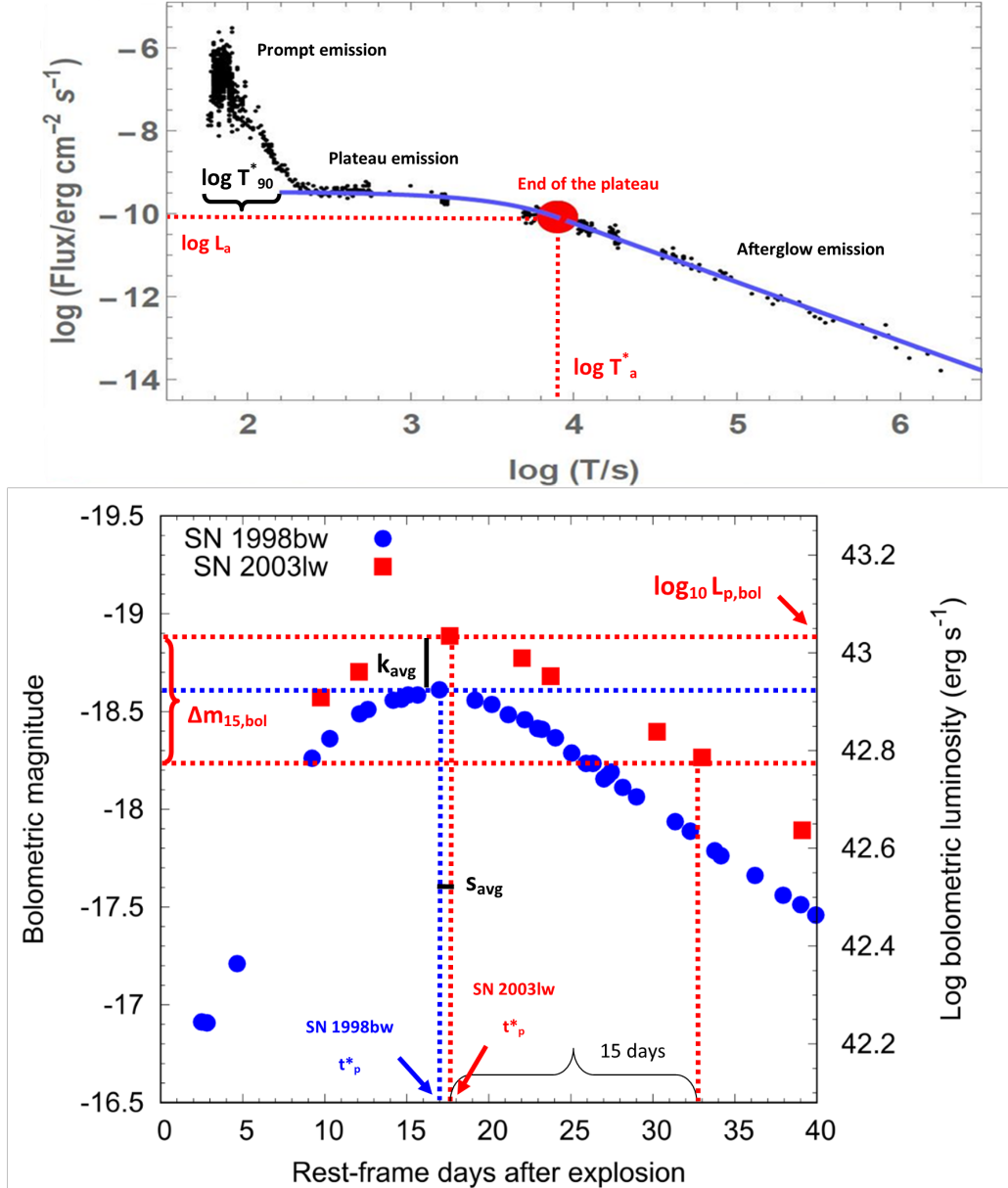


Figure 1. Upper panel. A schematic picture of a GRB LC in the rest frame with the main features. **Lower panel.** A plot where the properties of the SN LC in the case of association with a GRB are highlighted: we remind that the template LC is the one of SN 1998bw (colored in blue in the panel) while the examples of properties are referred to SN 2003lw.

Regarding the physical interpretation of the relations which involve the plateau emission, the so-called Dainotti 2-dimensional and 3-dimensional correlations, these have been interpreted as resulting from a newly born spinning down magnetar (Duncan 2001; Dall'Osso et al. 2011; Rowlinson et al. 2013; Rowlinson et al. 2014; Rea et al. 2015; Stratta et al. 2018) with an intense magnetic field ($B \sim 10^{14} \div 10^{15}$ G) or as the fallback accretion (Kumar et al. 2008a,b; Cannizzo & Gehrels 2009; Cannizzo et al. 2011). Within the first model, a magnetar powers the AG plateau phase and collapses into a BH at the end of this phase, transitioning into the power-law decline typically seen in late

AG LCs. In the second scenario, the Dainotti 2-dimensional relation suggests that the mass reservoir of the accretion disk is constant (Cannizzo et al. 2011). The prompt-afterglow plateau correlation has been interpreted within the standard fireball model accounting for a variation of the micro-physical parameters, see van Eerten (2014a,b). We can also refer to additional models which represent alternatives to these current ones, for example, the prior emission model (Yamazaki 2008) and the supercritical pile GRB model (Sultana et al. 2013).

The aforementioned relations concerning the GRB-SNe events are limited to the cross-relation of only GRB properties among themselves, without taking into account the SN observables. Indeed, the connection between GRB and SN properties has been highlighted in the other three relevant correlations, which are listed below. First, a correlation between the spectrum peak energy of the GRB, E_p , and the peak bolometric magnitude of the SN was found by Li (2006a): if an average luminosity SN has an accompanying GRB, the latter is expected to have soft spectra with a peak in the X-ray/UV wavelengths. The second is between the stretch, s , and luminosity factor, k , of SNe associated with GRBs (Cano 2014). This relation is similar to the peak luminosity-decline rate relationship (or Phillips relation, Phillips 1993) used to establish SNe Type Ia as standard candles. For a schematic picture of these quantities, see the lower panel of Figure 1.

The relation between the peak bolometric magnitude and E_p was also confirmed in Lü et al. (2018). From this relation, Lü et al. (2018) derive the one between E_p and the SN nickel mass (M_{Ni}) naturally, given the proportionality of the peak bolometric magnitude to M_{Ni} (Arnett 1982), but with a probability of non-correlated data $\sim 23\%$.

So far, only the above-mentioned few correlations have been investigated between the properties of GRBs and SNe, but with no restrictive metrics about the probability of chance occurrence. In addition, the quest for correlations in the GRB-SNe class has involved only the GRB prompt parameters to date. Thus, we propose an extensive search in the literature among 91 pairs of variables between GRBs and SNe parameters to seek possible new correlations, significantly leveraging the GRB plateau properties. We here stress that this work is focused on the search for new correlations between GRB and SNe parameters and not between the GRB-GRB and SN-SN relations.

In this way, the AG emission plays a central role in searching for GRB-SNe correlations. In general, this work aims to investigate newly found GRB-SNe correlations, to advance the goal of standardizing GRB-SNe giving clues on their emission mechanism, and advance towards the goal of their use GRBs as cosmological probes. More specifically, the more we know about the existence and reliability of the correlations, the more we can reveal and interpret their connection with the GRB emission mechanism. Once the phenomenon is known, then the variable which does not carry the information on the distance luminosity can be employed to use correlations as standard candles.

The paper is structured as follows: in Section 2 we present the observables pertinent both to GRBs and SNe to date; in Section 3.1, we describe the data samples, the further classification of the investigated events, and the data selection before the analysis; in Section 3.2 we show the results after the correction for selection biases and redshift evolution through the Efron & Petrosian method (hereafter called the EP method, Efron & Petrosian 1992); in Section 3.3 we introduce the metrics for the existence of the correlations; in Section 4, we provide the results of the analysis and we empirically discuss their possible physical interpretation. Finally, we conclude with a summary of findings in Section 5. In Appendix A the complete scatter matrices and all the possible cross-related pairs of variables are reported. We here report also the correlations with GRB-GRB and SN-SN parameters for completeness, although we do not study nor discuss them. In Appendix B we show the weighted fitting procedure with errors on both the variables. Lastly, in the Appendix C, we provide a more detailed introduction of the reliable statistical EP method, which allows for overcoming biases and selection effects in the newly found correlations.

2. NOTATIONS

For clarity, the nomenclature adopted in this paper is summarized in this Section. Together with the redshift of the GRB-SNe, we have gathered from the literature the values for 9 GRB parameters and 10 SN parameters.

- z : the redshift of the GRB-SN;
- T_{90}^* : the rest-frame time during which a GRB emits 90% of its energy, from 5% to 95%, expressed in s;
- $E_{\gamma,\text{iso}}, L_{\gamma,\text{iso}}$: the isotropic energy and luminosity of the GRB expressed in erg and erg/s, respectively;
- E_p^* : the peak spectral energy of the GRB, reported in keV, in the rest-frame: $E_p^* = E_p(1+z)$;
- $L_{\text{a,opt}}$: the luminosity at the end of the GRB plateau emission, observed in the optical wavelengths and measured in erg/s;

- $T_{\text{a,opt}}^*$: the rest-frame time at the end of the GRB plateau emission, observed in the optical wavelengths and measured in s;
- $L_{\text{a,X}}$: the luminosity at the end of the GRB plateau emission, observed in the X-rays and measured in erg/s;
- $T_{\text{a,X}}^*$: the rest-frame time at the end of the GRB plateau emission, observed in the X-rays and measured in s;
- θ_{jet} : the jet opening angle of the GRB estimated with the jet-break time, expressed in degrees ($^\circ$);
- T_{jet}^* : the rest-frame jet break time of the GRB, expressed in days;
- $L_{\text{p,bol}}$: the peak bolometric luminosity of the SN, measured in erg/s;
- $\Delta m_{15,\text{bol}}$: the magnitude decline of the SN 15 days after its peak in the bolometric LC, in mag, defined in the rest-frame (Cano et al. 2017a);
- t_{p}^* : the rest-frame time for the SN peak in the bolometric LC, after the GRB trigger, expressed in days;
- E_{K} : the kinetic energy of the SN, expressed in erg;
- M_{ej} : the ejecta mass of the SN, expressed in solar masses, M_{\odot} ;
- M_{Ni} : the mass of nickel-56 (^{56}Ni) produced in the SN explosion, expressed in M_{\odot} ;
- v_{ph} : the photospheric velocity of the SN, measured in km/s;
- k_{avg} : the luminosity factor of the SN, averaged between the different bands, and compared to the template 1998bw SN lightcurve;
- s_{avg} : the stretch factor of the SN, averaged between the different bands, and compared to the template 1998bw SN lightcurve.

The superscript (*) denotes that the quantity is estimated in the rest-frame only when the variables are not already by definition in the rest-frame, such as the GRB luminosities and isotropic energy. For example, concerning the time variables, we need to consider the cosmological evolution and divide by $(1+z)$, while we multiply by $(1+z)$ for peak energy. The superscript (') denotes the variable de-evolved when redshift evolution is removed. We mention that the redshift z is the only parameter common to the GRB and SN parameter sets.

Regarding the classes of GRBs, we here summarize the events pertinent to our analysis, and we quote their respective acronyms, which appear in Table 3:

- ULGRBs: the ultra-long GRBs, (Nakauchi et al. 2013; Virgili et al. 2013; Levan et al. 2014; Piro et al. 2014; Schady 2017; Perna et al. 2018; Moriya et al. 2020; Tsvetkova et al. 2021) with an unusual long duration, $T_{90}^* \geq 10^3$ s (Gendre et al. 2019);
- XRFs: the X-ray Flashes, for which the spectra is uncommonly soft and fluences in the X-ray band (2–30 keV) are bigger than the ones in the γ -ray (30–400 keV) band (Heise 2003; Sakamoto 2004; Gendre et al. 2007);
- llGRBs: low-luminosity events, where $L_{\gamma,\text{iso}} < 10^{48}$ erg/s (Liang et al. 2007; Virgili et al. 2009; Zhang et al. 2018a,b);
- INTs: the intermediate luminosity GRBs, where 10^{48} erg/s $< L_{\gamma,\text{iso}} < 10^{49.5}$ erg/s (Schulze et al. 2014; Cano et al. 2017a).

We here remind the reader that the rest of the GRBs with luminosities $L_{\gamma,\text{iso}} > 10^{49.5}$ erg/s are considered typical GRBs and indicated with the label GRBs. We briefly define the classes of SNe that are present in the current sample of GRB-SNe associations:

- SNe Ib: show no silicon nor hydrogen line, but include helium line in their spectra;

- SNe Ic: the silicon, hydrogen, and helium lines are absent; together with the Ib, these mostly originate from the death of massive stars;
- SNe Ic-BL (broad-lined Ic): Ic with broader lines than the usual Ic spectra (Chen et al. 2017; Modjaz et al. 2009);
- SLSNe (superluminous SNe): events that are around 100 times brighter than a Core-Collapse Supernova (CC SN) (Nicholl 2021; Tanaka et al. 2012).

In Figure 1, we show a schematic GRB picture showing the most relevant variables for GRBs (see the upper panel of Figure 1) and a plot of two SN LCs (the template SN 1998bw and the transient SN 2003lw) associated with GRBs where the parameters of the LC have been highlighted (see the lower panel of Figure 1).

In our example, we consider the SN 2003lw for the definition of the parameters, while the average stretch and luminosity factors, s_{avg} and k_{avg} , are shown concerning the template LC of SN 1998bw.

3. METHODOLOGY

This Section provides a complete description of the methods adopted to investigate the GRB-SNe correlations, describing the sample selection cut, the fitting procedures, and the selection bias corrections applied.

3.1. The data sample selection

To conduct our analyses, we searched the literature for GRB-SN associations and gathered reported properties for both components.

Of the hundreds of GRBs annually observed, only $\sim 2\text{-}7\%$ are spectroscopically or photometrically linked with SNe (Rossi et al. 2021). To date, ~ 40 GRB-SNe associations have been identified by LC bumps, while other independent 28 GRB-SNe associations (differently from the 40 SNe) have been spectroscopically confirmed. In many cases, the connection has been made by cross-checking the times and locations of GRBs and SNe in their respective catalogs (Wang & Wheeler 1998; Bosnjak et al. 2006), expanding to more than 100 possible associations.

Taking as our primary reference the GRB-SN events discussed in Cano et al. (2017a), our search uncovered 106 possible GRB-SN events spanning the 30-year time frame from 1991 to February 2021. It is important to stress that all the SN LCs associated with GRBs present in this sample consider the event SN 1998bw as the template. When we do not find out values in Cano et al. (2017a) we refer to other values tabulated in the literature referenced in Table 7. Concerning the v_{ph} parameter, when we do not find the uncertainty for the reported value, we substitute it with “-” in the Table 7, although a standard deviation $\sigma_{v_{\text{ph}}} = 8000 \text{ km/s}$ is reported in Cano et al. (2017a). This was estimated considering the distribution of the v_{ph} values. We also stress that we consider in the analysis only bolometric variables and not the ones in the given bands (e.g. the V-band absolute magnitude of the SN, M_V).

We report many SNe associated with GRBs in tables even if we do not have the associated estimated SN properties. We have reported them in any case since the associations that have only GRB properties are used to investigate the evolutionary effects through the statistical EP method. Thus, these tables are complete so that any reader can safely reproduce and compare the results. From the list of 106 probable associations, we remove 35 events due to the lack of data, the uncertain association, or the association with SNe II (and even with SN Ia). These latter associations with other spectroscopic classes than the Ib/c have arisen solely by a spatial and temporal coincidence of two different events and are based on old data (in the years ~ 1991), given that GRBs are associated with SNe Ib/c and not with SNe Ia nor SNe II.

Because of these uncertainties or unreliable observable parameters, the following 35 events were removed: GRB 920321/SN 1992Q, GRB 951107C/SN 1995bc, GRB 970514/SN 1997cy, GRB 971221/SN 1997ey, GRB 980525/SN 1998ce, GRB 980910/SN 1999E, GRB 990902/SN 1999dp, GRB 011121/SN 2001ke, GRB 920613/SN 1992ae, GRB 920628/SN 1992at, GRB 920708/SN 1992al, GRB 920925/SN 1992bg, GRB 930524/SN 1993R, GRB 950917/SN 1995ac, GRB 961029/SN 1996bx, GRB 970907/SN 1997dg, GRB 971218/SN 1998B, GRB 980503/SN 1998ck, GRB 990527/SN 1999ct, GRB 990719/SN 1999dg, GRB 990810, GRB 991015/SN 1999ef, GRB 991123/SN 1999gj, GRB 000319, GRB 000415/SN 2000ca, GRB 010921, GRB 020410, GRB 080503, GRB 090426, iPTF15dld, SN 2020bvc, GRB 210610B, GRB 211015A, GRB 211023A/AT 2021acco, and GRB 211211A (a recent transient associated with a Kilonova, Rastinejad et al. 2022).

Removing these GRBs leaves us with a total sample of 71 GRBs, tabulated in Table 7. This sample includes 58 associated GRB-SNe events according to the grading scheme of Hjorth & Bloom (2012). This scheme can be

summarized in 5 classes A,B,C,D, and E: Class A) have reliable spectroscopic evidence of the SNe; B) have a well-defined LC bump as well as some spectroscopic evidence resembling a GRB-SN; C) shows a bump which is evident and consistent with other GRB-SNe located at the spectroscopic redshift of the GRB; D) here a bump is present but the SN properties are not fully compatible with other GRB-SNe, or the bump is not well sampled or there is no spectroscopic redshift of the GRB; E) a bump, is either not significant or inconsistent with other GRB-SNe.

In the sample we have 9 A-graded, 4 AB-graded, 14 B-graded, 1 BC-graded, 11 C-graded, 1 CD-graded, 8 D-graded, 2 DE-graded, 8 E-graded events. The remaining 13 events included in the 71 GRBs sample are ungraded.

Previous studies have focused on A and B classes only (Lü et al. 2018).

In the current analysis, we retain all the possible GRB-SNe associations with sufficient data coverage. We also consider the plateau emission in the AG for 15 GRBs in the X-ray of the GRBs associated with SNe gathered in our sample. The luminosity at the end of the plateau emission is obtained through the LCs fitting with the Willingale model (Willingale et al. 2007), while the other parameters at play have been collected from the literature. In our sample, there are 15 and 20 GRBs with X-ray and optical plateau emission, respectively.

We found in our sample that the majority belong to the Ic class (17 events) and SNe Ic-BL (7 events), but there are several SNe Ib (3 events), and SNe with no clear distinction between Ib and Ic classes (5 events). We also have one single case of SLSN. After gathering all the properties for the reliable GRB-SNe associations, a further sample selection cut is performed by removing the two shock breakout events. The mechanisms for the production of LGRBs and shock breakout events are different: the former is likely generated from a collapsar, while the latter is probably linked to failed jets, namely events where the ultra-relativistic jets do not pierce into the stellar envelope and release their energy inside the progenitor, causing a relativistic shock breakout emission. The role of relativistic jets in the emission of GRB-SNe has been widely discussed in Aloy et al. (1999); Zhang & Woosley (2002); Umeda et al. (2005); Tominaga et al. (2007); Nomoto et al. (2008); Nagataki (2009); Granot & van der Horst (2014); Kumar & Zhang (2015); Eisenberg et al. (2022).

Two events, given their possible nature of shock breakouts, have been reported in our GRB-SNe sample but for the safety of separation from the other classes have been excluded from the analysis: GRB 060218/SN 2006aj (Campana et al. 2006; Ferrero et al. 2006; Pian et al. 2006; Soderberg et al. 2006b; Sollerman et al. 2006; Dainotti et al. 2007; Waxman et al. 2007; Campana et al. 2008; Zhang et al. 2022) and GRB 080109/SN 2008D (Li 2008a; Mazzali et al. 2008; Modjaz et al. 2009). The former has an energy many hundred times smaller than other cosmological GRBs, while the latter has an SN with relatively high energy if compared with the other CC SNe. For the other GRB-SNe events characterized by a relatively low luminosity, a consensus on their progenitor mechanism does not exist despite many of their features being typical of the shock breakout events. Indeed, a shock breakout scenario can be found also in GRBs that are not low luminous, like the case of GRB 120422A/SN 2012bz (Schulze et al. 2014), so this is not necessarily a typical behavior of the llGRBs. We here recall that the other events classified as llGRBs are GRB 980425/SN 1998bw (Galama et al. 1998; Pian et al. 2004), GRB 100316D/SN 2010bh (Starling et al. 2010), and GRB 171205A/SN 2017iuk (Barthelmy 2011; D'Elia et al. 2018; Suzuki et al. 2019). The subsequent analysis will be then performed on the sample of 69 GRB-SNe, removing the two shock breakouts GRB 060218/SN 2006aj and GRB 080109/SN 2008D from the aforementioned sample of 71 GRB-SNe associations.

In our sample, the GRB variables are affected by a mean ratio of errors over measurements $\Delta x_{GRB}/x_{GRB} \sim 21\%$, while the SN ones show larger relative errors leading to a mean $\Delta x_{SN}/x_{SN} \sim 39\%$. The extreme cases are the log-luminosity at the end of the optical GRB plateau with the smallest ratio in our sample ($\Delta \log_{10} L_{a,opt}/\log_{10} L_{a,opt} \sim 0.1\%$) and the SN kinetic energy with the largest relative uncertainties ($\Delta E_K/E_K \sim 94\%$). The details of these estimations are reported in Table 1: in the first column, we report the variable, in the second we report the mean of the ratios between the symmetrized 1σ errors and the values, while in the third column we report the number of data points involved in the estimation (namely, the number of events that have both the central value and the error for the given variable).

3.2. The application of the EP method to the variables

The EP method (Efron & Petrosian 1992) is a non-parametric method that involves an adapted version of Kendall's τ statistics (Kendall 1948). The method can be used to address the problem of the statistical dependence of the astrophysical variables on the redshift: in this way, the presence of hidden biases or selection effects for the investigated quantities can be revealed. Indeed, the EP could even reveal intrinsic correlations which would otherwise be hidden and masked out by the presence of redshift evolution and biases. On the other hand, the method can reveal if there

Variable	$\langle \Delta x/x \rangle$	N. of GRBs
T_{90}^*	15%	54
$E_{\gamma,\text{iso}}$	51%	51
E_p^*	52%	55
$\log_{10} L_{a,\text{opt}}$	0.1%	20
$\log_{10} T_{a,\text{opt}}^*$	1%	20
$\log_{10} L_{a,X}$	0.2%	15
$\log_{10} T_{a,X}^*$	2%	15
θ_{jet}	17%	16
T_{jet}^*	50%	16
$\log_{10} L_{p,\text{bol}}$	1%	22
E_K	94%	34
M_{ej}	58%	34
M_{Ni}	47%	36
v_{ph}	35%	22
k_{avg}	22%	35
s_{avg}	15%	33

Table 1. The table contains the variable name, the mean of relative errors for the variables, indicated with $\langle \Delta x/x \rangle$, and the number of GRBs present for each variable.

are correlations that are simply induced by selection biases and redshift evolution, and they are not intrinsic to the GRB physics.

More specifically, the EP method defines evolutionary functions, $g(z) = (1+z)^k$ where k is the evolutionary coefficient so that the new de-evolved variables indicated with ' will be divided by this function. Despite the continuous improvement of instruments, telescopes, and facilities with the subsequent enhanced precision and sensitivity in measurements, the biases still affect the data, given that each satellite has its instrumental selection effect. One of the principal biases is the so-called Malmquist bias (Malmquist 1922): according to this, at larger distances (or redshifts), it is easier to observe the more luminous objects rather than the fainter ones. The presence of biases in astrophysics affects also cosmological analysis (Dainotti et al. 2021b, 2022a), so it is important to tackle them.

The EP method's description is present in the Appendix C. We have applied it to several selected variables which are expected to undergo redshift evolution, both for GRB and SNe parameters. A complete correction of all the variables in the GRB-SNe sample can be found in Table 2. We here stress that we used the GRB-SNe sample to evaluate the evolutionary effects to allow the limiting variables, such as fluxes, times, or fluences sample to be as much as representative of the current sample. We also note that when the sample is small we use the full LGRBs class and the results of the evolutionary parameters are compatible within 1σ .

We here report the corrections related to variables found for t_p^* , which is one of the variables present in our correlations, while for v_{ph} there is no evolution. For the plateau properties in the X-rays and optical bands, in particular $L_{a,\text{opt}}$, the method does not allow precise estimates of the coefficients given the small sample related to the GRB-SN connection, so we adopt the values from a recent study in which the sample size is much larger, and we assume that the coefficients of the evolution do not change between the different samples (Dainotti et al. 2021a). Thus, we take the evolutionary coefficients as $k_{L_{a,\text{opt}}} = 3.96^{+0.58}_{-0.58}$. Concerning the T_{90}^* , the determined $k_{T_{90}^*} = -0.84^{+0.73}_{-0.67}$ is compatible in 1σ with the one of Lloyd-Ronning et al. (2019), thus validating our approach in the current analysis. For the variables M_{Ni} and M_{ej} we find $k_{M_{\text{Ni}}} = -0.07^{+0.77}_{-1.04}$ and $k_{M_{\text{ej}}} = -0.45^{+0.81}_{-0.52}$, respectively. Differently from the other variables, in the M_{Ni} and M_{ej} cases it is expected that no evolutionary effect is present: indeed, the coefficients are compatible with zero in 1σ . Thus, we simply report them in the Table 2 but in the subsequent analysis, we will assume $k_{M_{\text{Ni}}} = 0$ and $k_{M_{\text{ej}}} = 0$. Finally, for what it concerns the s_{avg} and k_{avg} parameters, an evolution is not expected and we will assume $k_{s_{\text{avg}}} = 0$, $k_{k_{\text{avg}}} = 0$; nevertheless, we performed a consistency check on the s_{avg} parameter since it is not unlikely that the stretch parameter may undergo a redshift evolution effect, as pointed out in Nicolas et al. (2021) for the SNe Ia. Thus, we estimated the following value of the correction parameter for the stretch: $k_{s_{\text{avg}}} = 0.16^{+0.21}_{-0.22}$. Being this value compatible with zero in less than 1σ , our assumption of $k_{s_{\text{avg}}} = 0$ is legit and will be taken into account for the rest of the analysis.

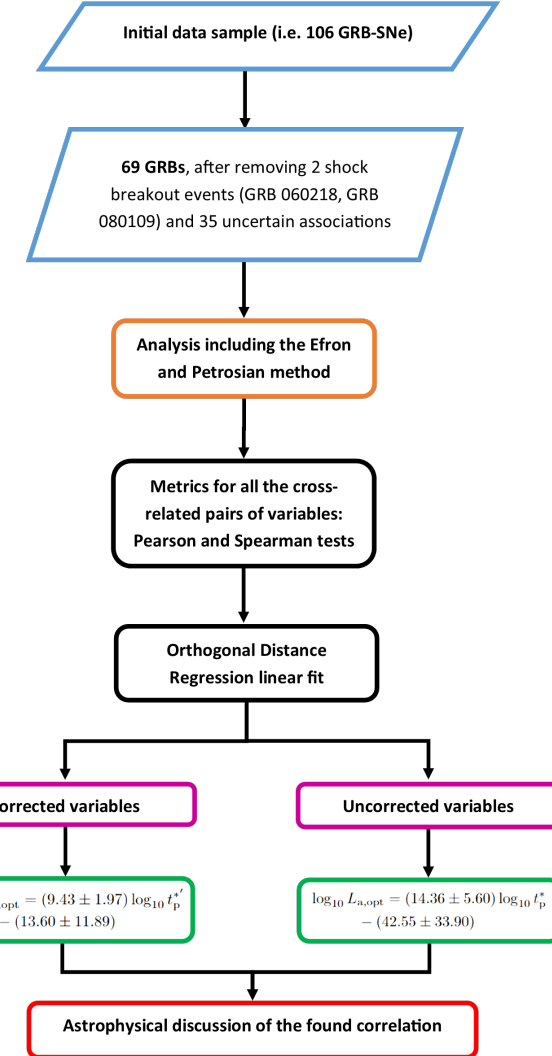


Figure 2. The flow chart here presented summarizes the steps of the current research for probable correlations in the sample of GRB-SNe associations.

The flowchart shown in Figure 2 explains the steps of this research and how the EP method enters into play.

3.3. The metrics of our analysis

This Section introduces the metrics and the statistical tests used for our analysis: the Pearson and the Spearman, as also shown in the third step of the flowchart in Figure 2. We will denote Pearson's correlation coefficient and p-value as r and P_P , respectively, while for Spearman's rank coefficient and p-value we will write ρ and P_ρ , respectively. The p-values P_P and P_ρ express the probability that the correlation may be drawn by chance, see for results Section 4. The Pearson correlation coefficient, r , (Pearson 1901) is a measure of how well a linear correlation can describe the data.

Spearman's ρ (Spearman 1904) measures how well a monotonic function can describe the relationship between two lists of data, basing the result on the rank differences.

The coefficients r and ρ both represent the correlation between the two distributions, and they both range from -1 to $+1$ (from the anticorrelation to the correlation case, respectively), but while the Pearson indicates the presence of a linear relation, the Spearman takes into account the ties and the ordering of the distribution, highlighting a monotonic function for the data, if present.

Both the Pearson and the Spearman have been performed with a null hypothesis \mathcal{H}_0 that the vectors are independent, and as the complementary hypothesis, \mathcal{H}_a that they are not. A small p-value suggests that it is improbable that \mathcal{H}_0

Quantity	EP coefficient	Symmetrized error	Computed in
T_{90}^*	$k_{T_{90}^*} = -0.78^{+0.89}_{-0.95}$	$\delta k_{T_{90}^*} = 0.92$	This paper
$E_{\gamma,\text{iso}}$	$k_{E_{\gamma,\text{iso}}} = 2.30 \pm 0.50$	$\delta k_{E_{\gamma,\text{iso}}} = 0.50$	Lloyd-Ronning et al. (2019)
$L_{\gamma,\text{iso}}$	$k_{L_{\gamma,\text{iso}}} = 3.50 \pm 0.50$	$\delta k_{L_{\gamma,\text{iso}}} = 0.50$	Lloyd-Ronning et al. (2019)
E_p^*	$k_{E_p^*} = 0.75 \pm 0.25$	$\delta k_{E_p^*} = 0.25$	Xu et al. (2021)
$L_{a,\text{opt}}$	$k_{L_{a,\text{opt}}} = 3.96 \pm 0.58$	$\delta k_{L_{a,\text{opt}}} = 0.58$	Dainotti et al. (2021a)
$T_{a,\text{opt}}^*$	$k_{T_{a,\text{opt}}^*} = -2.11 \pm 0.49$	$\delta k_{T_{a,\text{opt}}^*} = 0.49$	Dainotti et al. (2021a)
$L_{a,X}$	$k_{L_{a,X}} = 2.42 \pm 0.58$	$\delta k_{L_{a,X}} = 0.58$	Dainotti et al. (2021a)
$T_{a,X}^*$	$k_{T_{a,X}^*} = -0.85 \pm 0.30$	$\delta k_{T_{a,X}^*} = 0.30$	Dainotti et al. (2021a)
θ_{jet}	$k_{\theta_{\text{jet}}} = 0.75 \pm 0.25$	$\delta k_{\theta_{\text{jet}}} = 0.25$	Lloyd-Ronning et al. (2020)
T_{jet}^*	-	-	(*)
$L_{p,\text{bol}}$	$k_{L_{p,\text{bol}}} = 0.77^{+0.80}_{-0.25}$	$\delta k_{L_{p,\text{bol}}} = 0.52$	This paper
$\Delta m_{15,\text{bol}}$	-	-	(*)
t_p^*	$k_{t_p^*} = -0.43^{+0.19}_{-0.24}$	$\delta k_{t_p^*} = 0.22$	This paper
E_K	$k_{E_K} = -0.10^{+0.55}_{-0.90}$	$\delta k_{E_K} = 0.72$	This paper
M_{ej}	$k_{M_{\text{ej}}} = -0.45^{+0.81}_{-0.52}$	$\delta k_{M_{\text{ej}}} = 0.66$	This paper
M_{Ni}	$k_{M_{\text{Ni}}} = 0.07^{+0.77}_{-1.04}$	$\delta k_{M_{\text{Ni}}} = 0.90$	This paper
v_{ph}	-	-	(*)
k_{avg}	-	-	(*)
s_{avg}	$k_{s_{\text{avg}}} = 0.16^{+0.21}_{-0.22}$	$\delta k_{s_{\text{avg}}} = 0.22$	This paper

Table 2. Summarizing of the EP coefficients for the GRB-SNe parameters present in this paper. (*) means that the EP correction cannot be applied due to the paucity or the sparsity of the data.

is true; namely, it is unlikely that the two vectors are independent. In other words, if they are not independent, the smaller the p-value, the higher the probability that the correlation is not drawn by chance. We assess the presence of the correlations with the metrics indicated by the Pearson and/or Spearman correlation and their relative probability that the correlation is driven by chance. Specifically, the correlations must fulfill at least one of the two following conditions: (I) $|r| \geq 0.50$ and $P_P \leq 0.05$ for the Pearson's test, and/or (II) $|\rho| \geq 0.50$ and $P_\rho \leq 0.05$ for the Spearman's test.

We here remind the reader that this work is focused on the search for new correlations between GRB and SNe parameters and not between the GRB-GRB and SN-SN relations. Thus, we limit ourselves to reporting the GRB-GRB and the SN-SN in Table 5 for the cases without EP-correction and in Table 6 for the cases that include the EP-correction without further discussing their physical meaning, since the majority of them have been discussed in the literature already. Despite many of the GRB-SN relations satisfying the criteria (I) and/or (II), we do not investigate them due to the paucity of data (less than 5 data points) or the absence of the EP-correction coefficient for one of the variables. The GRB-SNe relations which fulfill the metrics, but have not been discussed, are $\Delta m_{15,\text{bol}} - \log_{10} T_{\text{jet}}^*$ (both with and without EP-correction) since the correlation is drawn by only 3 data points, $\log_{10} v_{\text{ph}} - \log_{10} \theta'_{\text{jet}}$, and $\log_{10} v_{\text{ph}} - \log_{10} L_{\gamma,\text{iso}}'$ since the v_{ph} variable has no EP-correction coefficient. Nevertheless, we cannot exclude a priori the existence of these correlations that may be, indeed, confirmed with the future observations of GRB-SNe.

In all the analyses we tested the criteria (I) and (II) and we did not find any candidate correlation that fulfills criterion (II). However, since the Tables 5, 6 show all the relations, we present anyway the analysis performed with this criterion giving in the table both the Pearson and Spearman correlation coefficients. Using the sample of 69 GRB-SNe, we begin our analysis by comparing each property of the GRB-SN sample against every other. To this end, we cross-correlate all the variables and we compute the correlation coefficients r , P_r , ρ , and P_ρ through the *scipy.stats* module².

After the metrics have been fulfilled we need to determine the slope and the normalization through a fitting procedure. For the correlations which respect at least one condition between (I) and (II) we perform a weighted linear regression (namely, with the model $y = ax + c$, being a the slope of the correlation and c the intercept), using the Orthogonal

² For Python package SciPy, see <https://docs.scipy.org/doc/scipy/reference/generated>

Distance Regression method (hereafter ODR, Boggs & Donaldson 1989). The ODR method deals with the problem of best fitting for data when the uncertainties are present not only on the dependent variable but also on the independent variable. For a quick introduction to the ODR method, see Appendix B. The ODR regression is performed with the `scipy.odr` package³. The error on each of the variables involved in the ODR fitting is estimated through the formula of error propagation, involving the uncertainties related to the EP evolutionary coefficients together with the 1σ uncertainties of the variables, when present.

It is important to discuss the impact of the errors in the analysis of the candidate correlation. All the GRB plateau observables in our sample are affected by errors $< 2\%$ (see Table 1), thus enforcing the reliability of the results in the research of the correlation between the SN and the GRB AG properties. It must be stressed that the uncertainties of the variables do not affect the metrics of our analysis and, thus, do not affect the identification of possible new correlations. This is due to the fact that to perform the Pearson and Spearman tests, we consider the central values of the parameters and not their uncertainties, focusing the subsequent investigation on the possible correlations that satisfy criterion (I).

The ODR fitting is applied to the following cases for each correlation: the sample with all the GRBs that obey the found correlations and the subsample of the correlations containing only the A, AB, and B-graded events, the so-called AB subsample. It is important to focus on correlations fulfilled by a sufficient number of at least 5 data points. We summarize in Table 3 the values of the parameters which show a clear correlation. In Appendix A, we report the results of the cross-checking for all the possible pairs of variables present in our GRB-SNe sample. The Pearson and Spearman coefficients for the tested pairs of the EP-corrected parameters are reported in the Appendix A, together with the tables mentioned above containing the cases without the EP corrections.

All the steps of the current analysis are summarized in the flow chart of Figure 2. Although it is important to stress that the relevant correlations are the ones that have been corrected for selection effects and redshift evolution, in this work we report also the correlations found in the cases with the observed variables without the EP-correction and the hybrid cases where the EP correction is present only for one of the variables in each pair. In this way, we provide a useful reference for future comparison between the corrected and uncorrected correlations.

³ For the SciPy ODR package, see <https://docs.scipy.org/doc/scipy/reference/odr.html>

Table 3. GRB-SNe parameters present in our correlations

GRB ID	SN ID	GRB Type	SN Type	$\log_{10} L_{\text{a, opt}}$	t_{p}^*
				(erg/s)	(days)
910423	1991aa	...	Ib
960221	1996N	...	Ib
960925	1996at	...	Ic-Ib/c
961218	1997B	...	Ic-Ib/c
970228	...	GRB
970508	Ib/c	...	16.79 ± 3.30
971013	1997dq	...	Ib
971115	1997ef	...	Ic
971120	1997ei	...	Ic
980326	...	GRB
980425	1998bw	IIGRB	Ic	...	15.16
980703
990712	...	GRB
991002	1999eb
991021	1999ex	...	Ic
991208	...	GRB
000114	2000C	...	Ic
000418
000911	...	GRB
020405	...	GRB
020903	...	IIGRB
021211	2002lt	GRB	Ic
030329	2003dh	GRB	Ic-BL	44.11 ± 0.09	12.75
030723	...	XRF
031203	2003lw	INT	Ic	...	17.33
040924	...	GRB	...	45.26 ± 0.13	...
041006	...	GRB	...	44.76 ± 0.07	...
050416A	...	GRB	...	43.70 ± 0.08	...
050525A	2005nc	GRB	Ic	45.51 ± 0.04	...
050824	...	GRB	...	44.87 ± 0.06	...
060218	2006aj	IIGRB	Ic-BL
060729	...	GRB	...	44.88 ± 0.03	...
060904B	...	GRB	...	45.25 ± 0.05	...
070419A	...	INT	...	45.05 ± 0.14	...
071025	11.9
071112C

Table 3 continued on next page

Table 3 (*continued*)

GRB ID	SN ID	GRB Type	SN Type	$\log_{10} L_{\alpha, \text{opt}}$	t_{p}^*
080109	2008D	XRF	Ib	...	12
080319B	...	GRB
081007A	2008hw	GRB	Ic	43.98 ± 0.10	15
090618	...	GRB	...	45.17 ± 0.01	8.76
091127	2009nz	GRB	Ic-BL	44.83 ± 0.04	...
100316D	2010bh	HGRB	Ic	42.06 ± 0.11	11.8
100418A	...	GRB	...	44.19 ± 0.12	...
101219B	2010ma	GRB	Ic	44.97 ± 0.02	...
101225A	...	ULGRB	...	42.43 ± 0.06	22.7
111209A	2011kl	ULGRB	SLSN	45.10 ± 0.08	14.45
111211A	13.6
111228A	...	GRB	...	45.52 ± 0.01	...
120422A	2012bz	GRB	Ic
120714B	2012eb	INT	Ib/c	...	13
120729A	...	GRB	12.94
130215A	2013ez	GRB	Ic	...	11.9
130427A	2013cq	GRB	Ic
130702A	2013dx	INT	Ic	43.59 ± 0.02	...
130831A	2013fu	GRB	Ib/c	45.52 ± 0.03	...
140206A
140606B	iPTF14bfu	GRB	Ic-BL
150818A	...	INT
161219B	2016jca	INT	Ic
161228B	iPTF17cvw	...	Ic-BL
171010A	2017htp	...	Ic-BL
171205A	2017iuk	...	Ic-BL
180720B
180728A	2018fip	XRF	Ic
190114C	2019irj
190829A	2019oyw	...	Ic-BL
200826A	...	GRB
210210A	...	GRB

4. AN HINT OF THE RELATION BETWEEN $L_{\text{a,opt}}$ AND t_p^* ?

We here present the results of the only possible correlation we found in our analysis: $\log_{10} L'_{\text{a,opt}}$ vs. $\log_{10} t_p^{* \prime}$. We point out that this correlation fulfills only the criterion that reports $|r| \geq 0.50$ and $P_P \leq 0.05$, namely the condition (I). For this correlation, the EP correction coefficient exists for both variables, thus allowing the subsequent analysis of the $\log_{10} L_{\text{a,opt}} - \log_{10} t_p^*$ relation. Furthermore, being this relation drawn by more than 5 data points, it can be further tested.

Our sample includes 9 GRB-SN events for which both $L_{\text{a,opt}}$ and t_p^* values were reported in the literature. The 9 GRB-SN events present in this correlation are: GRB 030329/SN 2003dh (Ic/HN), GRB 081007A/SN 2008hw (Ic), GRB 091127/SN 2009nz (Ic-BL), GRB 100316D/SN 2010bh (Ic), GRB 101219B/SN 2010ma (Ic), GRB 111209A/SN 2011kl (SLSN), GRB 111228A, GRB 130702A/SN 2013dx (Ic), and GRB 130831A/SN 2013fu (Ib/c). The fitting equation for the EP-corrected full sample is the following:

$$\log_{10} L'_{\text{a,opt}} = (9.43 \pm 1.97) \log_{10} t_p^{* \prime} - (13.60 \pm 11.89), \quad (1)$$

while for the EP-corrected AB subsample, the fitting EP-corrected equation is

$$\log_{10} L'_{\text{a,opt}} = (10.80 \pm 1.98) \log_{10} t_p^{* \prime} - (21.74 \pm 11.93). \quad (2)$$

The full sample case shows the Pearson's correlation coefficient $r = 0.71$ and a p-value of $P_P = 0.03$ in the EP-corrected case with the full sample fitting. Regarding instead the AB sample, Pearson's correlation coefficient is $r = 0.75$ and its p-value is $P_P = 0.03$. The fitting parameters for this correlation are reported in Table 4.

Fitting without the EP method			
Sample	ODR method	r	P _P
Full	$(14.36 \pm 5.60)x + (-42.55 \pm 33.90)$	0.70	0.04
AB only	$(21.50 \pm 8.82)x + (-85.36 \pm 53.14)$	0.70	0.05
Fitting with the EP method			
Sample	ODR method	r	P _P
Full	$(9.43 \pm 1.97)x + (-13.60 \pm 11.89)$	0.71	0.03
AB only	$(10.80 \pm 1.98)x + (-21.74 \pm 11.93)$	0.75	0.03

Table 4. The fitting parameters of the correlation $\log_{10} L_{\text{a,opt}} - \log_{10} t_p^*$ in the cases without and with the EP correction. The columns, from left to right, contain the sample, the ODR method fitting, Pearson's correlation coefficient r , and Pearson's p-value P_P . The fitting relations are expressed as: $y = (a \pm \sigma a)x + (c \pm \sigma c)$, where $x = \log_{10} t_p^*$, $y = \log_{10} L_{\text{a,opt}}$, $a \pm \sigma a$ is the slope with its error, and $c \pm \sigma c$ is the intercept with its error.

We here note that this correlation contains all the points from the AB sample together with an E-graded event (GRB 111228A), which draws the correlation together with the other present data points. This correlation is plotted in Figure 3. This correlation exists by evaluating the flatness of the slope in 5.4σ when we consider the entire sample and 4.7σ when we consider the AB sample.

4.1. The physical discussion of the $\log_{10} L_{\text{a,opt}} - \log_{10} t_p^*$ and the other relevant correlations

The peak time of a SN can be connected to the diffusion time through the Arnett model (Arnett 1982, see Cano 2011 for the implementation of the cobalt contribution):

$$L(t) = M_{\text{Ni}} e^{-x^2} \left((\epsilon_{\text{Ni}} - \epsilon_{\text{Co}}) \int_0^x 2k e^{-2ky+k^2} dk + \int_0^x 2k e^{-2ky+2ks+k^2} dk \right) \quad (3)$$

where $x \equiv t/\tau_m$, $y \equiv \tau_m/(2\tau_{\text{Ni}})$, $s = (\tau_m(\tau_{\text{Co}} - \tau_{\text{Ni}})/(2\tau_{\text{Co}}\tau_{\text{Ni}}))$, and $\tau_m = (k/\beta c)^{1/2} (M_{\text{ej}}^3/E_K)^{1/4}$ is the effective diffusion time, given the opacity $k = 0.07 \text{ cm}^2 \text{ g}^{-1}$. It is important to stress that, in the Arnett formulation, the diffusion time τ_m is proportional to the peak time t_p^* with a multiplying factor that depends on the temperatures and the opacity (Khatami & Kasen 2019). Thanks to this property, given the found correlation between $L_{\text{a,opt}}$ and t_p^* , we can expect the brightest GRB optical plateaus to be connected with the longer diffusion times of the associated SNe.

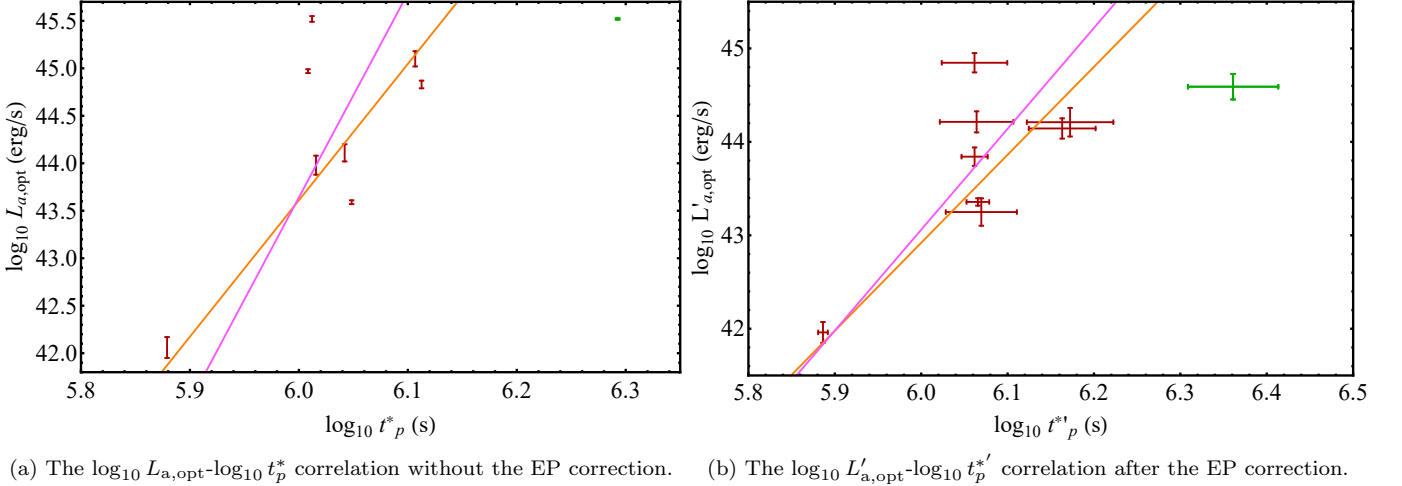


Figure 3. (a) The correlation between $\log_{10} L_{a,\text{opt}}$ and $\log_{10} t_p^*$ before the EP correction. (b) The correlation between $\log_{10} L'_{a,\text{opt}}$ and $\log_{10} t_p^{*'}$ after correcting both the variables with the EP method. The color-coded is the following: red refers to the AB subsample and green to the remaining E-graded event (GRB 111228A). For the fitting lines, orange indicates the full sample fitting and magenta the AB subsample fitting. The lines correspond to the fitting with ODR method parameters.

Other probable correlations have been highlighted between the SN v_{ph} and the GRB θ_{jet} and between v_{ph} and the GRB $L_{\gamma,\text{iso}}$ but, in these cases, since the photospheric velocity v_{ph} had no correction for selection biases through the EP method (see Section 3.2), it was not possible to achieve a reliable comparison between the uncorrected and corrected versions, being only θ_{jet} and $L_{\gamma,\text{iso}}$ corrected in the correlation. So, we retained only the probable correlation $\log_{10} L'_{a,\text{opt}}-\log_{10} t_p^*$ for further testing.

Finally, we would like to discuss the relevance of the correlation between E_p and M_{Ni} (Lü et al. 2018): in the case without the EP-correction, the Pearson correlation coefficient and p-value are $r = 0.33$ and $P_P = 0.06$, respectively, while for the Spearman we have $\rho = 0.31$ and $P_\rho = 0.08$, respectively. In the EP-corrected analysis, this relation shows $r = 0.34$ and $P_P = 0.05$ for the Pearson test, while $\rho = 0.34$ and $P_\rho = 0.05$ for the Spearman. Comparing our results with the ones from (Lü et al. 2018), these values show that the correlation coefficient (considering the EP-corrected case) drops from $r = 0.77$ (in Lü et al. 2018) to 0.34 (our results). This indicates a percentage decrease of 56% in r , while the p-values in our cases are smaller ($P_P = 0.05$ and $P_\rho = 0.05$), thus having a percentage decrease of 78% in our results. These new results have been achieved with a sample size of 33 GRBs vs. the 20 GRBs used in Lü et al. (2018), thus increasing the sample size by 40%. The fact that the p-value of this correlation drops substantially encourages the analysis of this correlation with the forthcoming GRB-SNe events in the next few years. However, we remark that the correlation coefficients from Pearson and Spearman tests in the EP-corrected case are $r = 0.34$ and $\rho = 0.34$, respectively: this is the reason why this correlation has not been presented as the main result since it does not fulfill our metrics.

5. SUMMARY AND CONCLUSIONS

This research aims to study the GRB-SN connection with the largest possible sample of physical variables presented in the literature. To this end, we compiled an extensive collection of GRB-SN properties and searched for correlations, see Appendix A for the scatter matrix plots of all the variables. More specifically, we have analyzed 9 and 10 variables among the SNe and GRB properties, respectively. We have tested 91 bi-dimensional correlations among GRB and SN properties for parameters both in the cases without and with selection biases corrections. For completeness, we have reported a total of 171 correlations which also include GRB-GRB and SN-SN correlations investigated with their Pearson, Spearman, and their probability to be drawn by chance, both in the cases without and with EP correction (see Table 5 and 6, respectively).

Indeed, the novelty of our approach compared to other previous works in the literature is that we apply a reliable statistical method, the EP method, to overcome selection biases due to instrumental thresholds and redshift evolution, which otherwise would remain hidden within the correlations. In addition, we have also applied two metrics for

selecting the correlations before and after the EP method. To summarize, only a correlation revealed with the metrics in (I), namely $|r| \geq 0.50$ and $P_P \leq 0.05$ for the Pearson, has been found.

We unveil a probable correlation between the optical luminosity at the end of the plateau emission and the rest-frame peak time of the SN. This correlation holds for a sample of 9 GRB-SNe and suggests that the SNe with a larger rest-frame peak time accompany the brightest GRB optical plateau emissions. Furthermore, the SNe with a later peak rising is associated with longer diffusion times, thus connecting the GRB optical plateau luminosity with the scaling of the SN LC. Thus, brighter GRBs at the end of the optical plateau emission are characterized by a larger diffusion time in their associated SNe. The slope of this correlation is non-zero at 5.4σ for the full sample and at 4.8σ for the AB sample. As a general remark, this correlation yields, however for small sample size, thus a larger sample is needed to secure our conclusions further. With such a future enlarged sample in our hands, we will be able to cast light on the GRB-SNe diversity and on the models that describe the progenitor of GRB-SNe.

Currently, no further significant correlations have been highlighted with these metrics. A possible reason for which other correlations that may be expected have not been found is the wide-spanning of the GRB prompt parameters, in many orders of magnitude with respect to the SNe parameters. Here we refer especially to the GRB prompt isotropic energy vs. the peak bolometric luminosities of the associated SNe. While the GRB isotropic energy can be observed between $10^{47}erg$ and $10^{54}erg$ for GRBs associated with SNe, the peak bolometric luminosities of the associated SNe remain in the order of $10^{52} - 10^{53}erg s^{-1}$, showing that is unlikely for a correlation to be present between the two parameters (Della Valle et al., 2022 in prep.). The same argument applies in the comparison between the isotropic energy of the GRB and the SN peak time, the latter being in the order of 10^6s . In view of these considerations, it's clear that the AG parameters in contrast to the prompt emission-only parameters, deserve a central role in the process of looking for correlations.

The metrics adopted here are stricter than previous metrics used in the literature. We point out hints about the existence of a new correlation in the GRB-SNe connections. The important key result is that the found correlation is intrinsic and not merely due to the result of selection effects or redshift evolution since we have tested it through the EP method.

We also point out that the correction for selection biases and redshift evolution, performed for the first time in the literature for this GRB-SNe sample, allows estimating the intrinsic behavior of physical parameters.

Indeed, our method of cross-correlating all quantities in principle could have revealed new correlations after applying the EP method, which otherwise would have remained hidden. In summary, this study paves the way to a) a broad investigation among all the existing parameters in the literature for both the SNe and GRBs; b) the use of reliable statistical methods to pinpoint possible hidden correlations; c) showing the challenge in finding new correlations given the paucity of the data we currently have at our disposal.

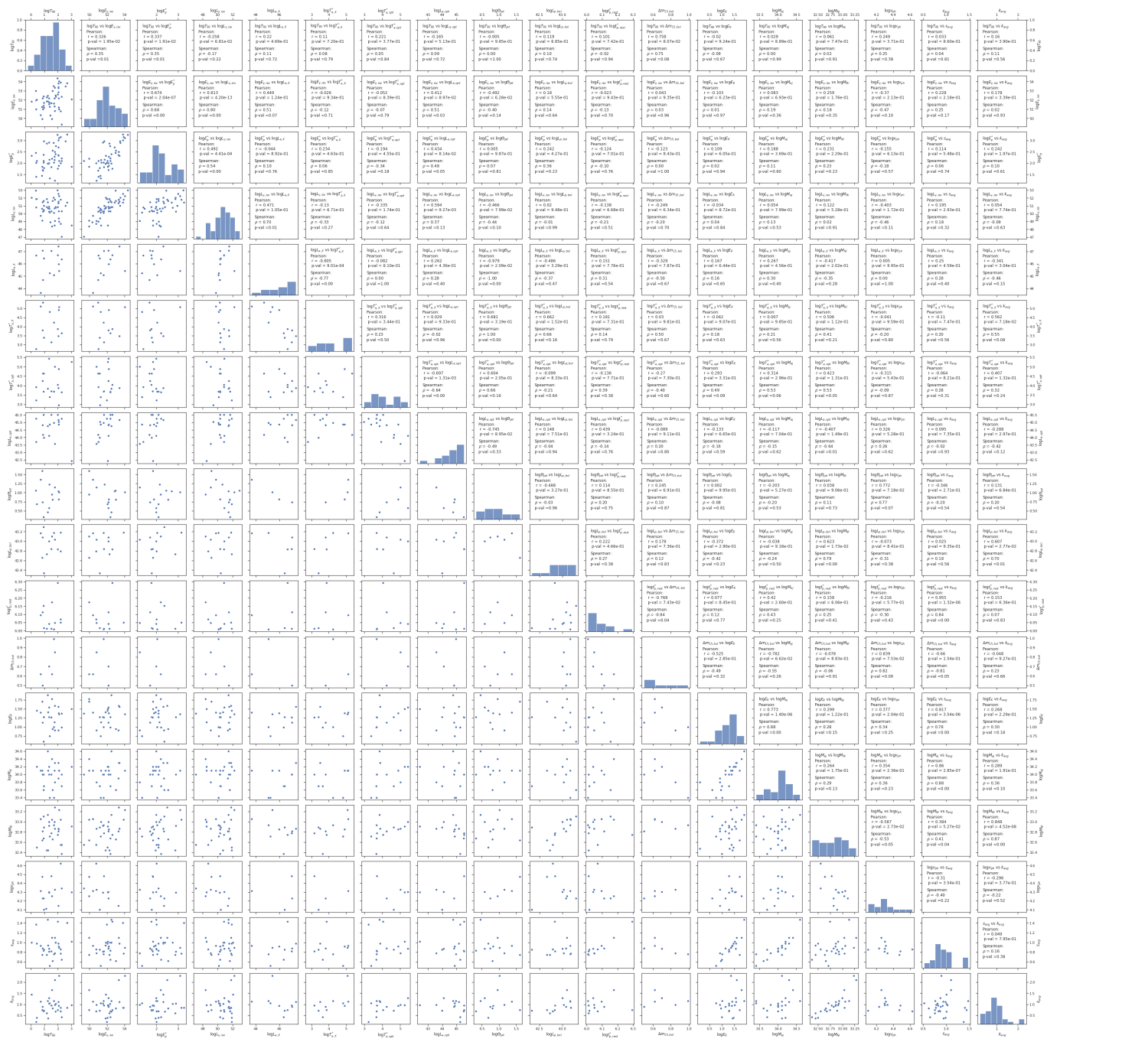
ACKNOWLEDGMENTS

This work was partly supported by the U.S. Department of Energy, Office of Science, Office of Workforce Development for Teachers and Scientists (WDTs) under the Science Undergraduate Laboratory Internships (SULI) program. This work used data supplied by the UK Swift Science Data Centre at the University of Leicester. We are grateful to Nicki O'Shea for the data collection and analysis performed during the SULI program. In the end, we would like to thank Dr. Enrique Cuellar (\dagger) for the kindness and availability he proved to have during his career: without him, there would not have been such a fundamental collaboration with the SULI program.

Appendices

A. SCATTER MATRICES AND TABLES

In this Appendix, we report the complete versions of the scatter matrices, namely Figure 4 for the cases without EP and Figure 5 for the cases including EP. We here also report the full tables with all the pairs of cross-related parameters. For the cases without the EP corrections, Table 5 summarizes the Pearson and Spearman's coefficients for each pair of variables between GRB and SN properties. Concerning the cases where the EP corrections are included, Table 6 contains the Pearson and Spearman's coefficients between GRB and SN properties.



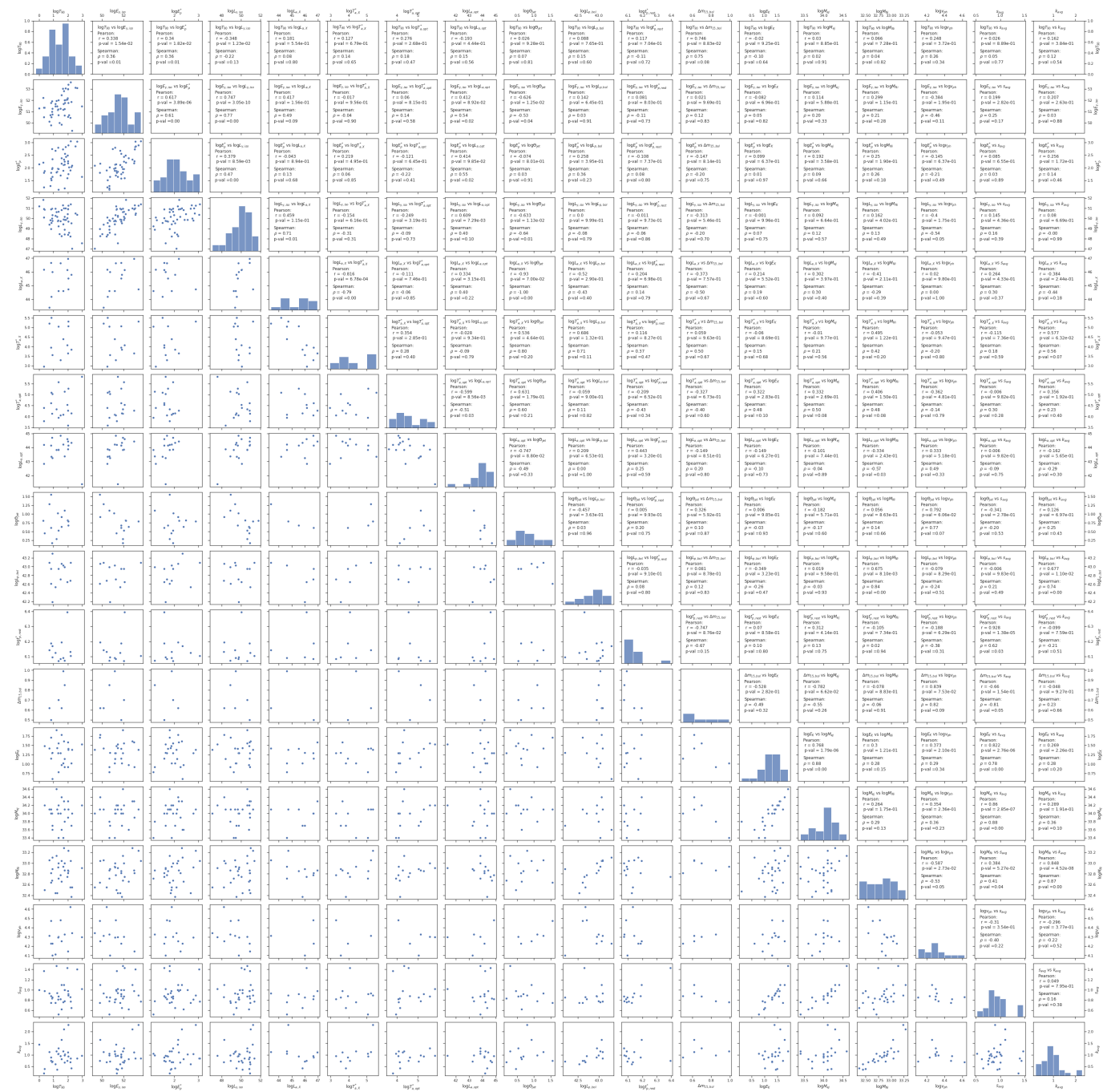


Figure 5. The scatter matrix with the EP-corrected variables, removing only the two shock breakout events (GRB 060218/SN 2006aj and GRB 080109/SN 2008D). For brevity, we here write log in place of \log_{10} .

Table 5. The cross-relation of GRB and SN observables in the case without the EP correction.

Relation	r	P_P	ρ	P_ρ	Notes	N. of points	Relation	r	P_P	ρ	P_ρ	Notes	N. of points
$\log_{10} T_{90}^*$ vs. $\log_{10} E_{\gamma,\text{iso}}$	0.3	0.03	0.34	0.01	5	54	$\log_{10} T_{90}^*$ vs. $\log_{10} E_p^*$	0.25	0.08	0.27	0.06	5	52
$\log_{10} E_{\gamma,\text{iso}}$ vs. $\log_{10} E_p^*$	0.7	< 0.01	0.72	< 0.01	2	50	$\log_{10} T_{90}^*$ vs. $\log_{10} L_{\gamma,\text{iso}}$	-0.36	0.01	-0.27	0.04	5	55
$\log_{10} E_{\gamma,\text{iso}}$ vs. $\log_{10} L_{\gamma,\text{iso}}$	0.82	< 0.01	0.78	< 0.01	5	54	$\log_{10} E_p^*$ vs. $\log_{10} L_{\gamma,\text{iso}}$	0.55	< 0.01	0.57	< 0.01	4	51
$\log_{10} T_{90}^*$ vs. $\log_{10} L_{\text{p,bol}}$	0.32	0.21	0.19	0.47	-	17	$\log_{10} E_{\gamma,\text{iso}}$ vs. $\log_{10} L_{\text{p,bol}}$	0.35	0.2	0.29	0.3	-	15
$\log_{10} E_p^*$ vs. $\log_{10} L_{\text{p,bol}}$	0.41	0.12	0.39	0.13	7	16	$\log_{10} L_{\gamma,\text{iso}}$ vs. $\log_{10} L_{\text{p,bol}}$	0.13	0.62	0.07	0.8	-	16
$\log_{10} T_{90}^*$ vs. $\log_{10} t_p^*$	-0.18	0.51	-0.08	0.76	-	16	$\log_{10} E_{\gamma,\text{iso}}$ vs. $\log_{10} t_p^*$	-0.06	0.83	-0.15	0.61	-	14
$\log_{10} E_p^*$ vs. $\log_{10} t_p^*$	0.11	0.71	0.06	0.82	-	15	$\log_{10} L_{\gamma,\text{iso}}$ vs. $\log_{10} t_p^*$	0.17	0.54	-0.1	0.72	-	15
$\log_{10} L_{\text{p,bol}}$ vs. $\log_{10} t_p^*$	0.3	0.26	0.37	0.15	-	16	$\log_{10} T_{90}^*$ vs. $\Delta m_{15,\text{bol}}$	0.48	0.19	0.53	0.14	-	9
$\log_{10} E_{\gamma,\text{iso}}$ vs. $\Delta m_{15,\text{bol}}$	-0.03	0.94	-0.07	0.86	-	8	$\log_{10} E_p^*$ vs. $\Delta m_{15,\text{bol}}$	-0.16	0.71	-0.24	0.57	-	8
$\log_{10} L_{\gamma,\text{iso}}$ vs. $\Delta m_{15,\text{bol}}$	-0.42	0.26	-0.38	0.31	-	9	$\log_{10} L_{\text{p,bol}}$ vs. $\Delta m_{15,\text{bol}}$	-0.15	0.7	-0.18	0.65	-	9
$\log_{10} t_p^*$ vs. $\Delta m_{15,\text{bol}}$	-0.63	0.07	-0.65	0.06	-	9	$\log_{10} T_{90}^*$ vs. $\log_{10} E_K$	0.08	0.68	-0.04	0.83	-	30
$\log_{10} E_{\gamma,\text{iso}}$ vs. $\log_{10} E_K$	-0.06	0.78	0.03	0.87	-	28	$\log_{10} E_p^*$ vs. $\log_{10} E_K$	0.09	0.63	0.07	0.71	-	29
$\log_{10} L_{\gamma,\text{iso}}$ vs. $\log_{10} E_K$	-0.03	0.87	-0.02	0.93	-	29	$\log_{10} L_{\text{p,bol}}$ vs. $\log_{10} E_K$	-0.1	0.75	-0.08	0.79	-	13
$\log_{10} t_p^*$ vs. $\log_{10} E_K$	0.17	0.6	0.24	0.46	-	12	$\Delta m_{15,\text{bol}}$ vs. $\log_{10} E_K$	-0.4	0.28	-0.49	0.18	-	9
$\log_{10} T_{90}^*$ vs. $\log_{10} M_{\text{ej}}$	-0.13	0.51	-0.12	0.53	-	30	$\log_{10} E_{\gamma,\text{iso}}$ vs. $\log_{10} M_{\text{ej}}$	-0.07	0.73	0.0	0.99	-	28
$\log_{10} E_p^*$ vs. $\log_{10} M_{\text{ej}}$	0.07	0.71	0.03	0.87	-	29	$\log_{10} L_{\gamma,\text{iso}}$ vs. $\log_{10} M_{\text{ej}}$	0.05	0.79	0.08	0.67	-	29
$\log_{10} L_{\text{p,bol}}$ vs. $\log_{10} M_{\text{ej}}$	-0.02	0.94	-0.15	0.62	-	13	$\log_{10} t_p^*$ vs. $\log_{10} M_{\text{ej}}$	0.47	0.12	0.47	0.12	-	12
$\Delta m_{15,\text{bol}}$ vs. $\log_{10} M_{\text{ej}}$	-0.73	0.02	-0.7	0.04	-	9	$\log_{10} E_K$ vs. $\log_{10} M_{\text{ej}}$	0.73	< 0.01	0.81	< 0.01	-	32
$\log_{10} T_{90}^*$ vs. $\log_{10} M_{\text{Ni}}$	0.13	0.48	0.06	0.72	-	34	$\log_{10} E_{\gamma,\text{iso}}$ vs. $\log_{10} M_{\text{Ni}}$	0.26	0.16	0.23	0.21	-	32
$\log_{10} E_p^*$ vs. $\log_{10} M_{\text{Ni}}$	0.33	0.06	0.31	0.08	6	33	$\log_{10} L_{\gamma,\text{iso}}$ vs. $\log_{10} M_{\text{Ni}}$	0.18	0.32	0.05	0.78	-	33
$\log_{10} L_{\text{p,bol}}$ vs. $\log_{10} M_{\text{Ni}}$	0.69	< 0.01	0.82	< 0.01	-	17	$\log_{10} t_p^*$ vs. $\log_{10} M_{\text{Ni}}$	0.43	0.1	0.43	0.1	-	16
$\Delta m_{15,\text{bol}}$ vs. $\log_{10} M_{\text{Ni}}$	-0.25	0.51	-0.36	0.34	-	9	$\log_{10} E_K$ vs. $\log_{10} M_{\text{Ni}}$	0.34	0.06	0.34	0.05	-	32
$\log_{10} M_{\text{ej}}$ vs. $\log_{10} M_{\text{Ni}}$	0.26	0.15	0.27	0.13	-	32	$\log_{10} T_{90}^*$ vs. $\log_{10} v_{\text{ph}}$	0.34	0.17	0.47	0.05	-	18
$\log_{10} E_{\gamma,\text{iso}}$ vs. $\log_{10} v_{\text{ph}}$	-0.17	0.54	-0.24	0.38	-	15	$\log_{10} E_p^*$ vs. $\log_{10} v_{\text{ph}}$	-0.24	0.37	-0.19	0.49	-	16
$\log_{10} L_{\gamma,\text{iso}}$ vs. $\log_{10} v_{\text{ph}}$	-0.4	0.13	-0.44	0.09	x	16	$\log_{10} L_{\text{p,bol}}$ vs. $\log_{10} v_{\text{ph}}$	-0.13	0.66	-0.3	0.31	-	13
$\log_{10} t_p^*$ vs. $\log_{10} v_{\text{ph}}$	-0.48	0.12	-0.5	0.1	-	12	$\Delta m_{15,\text{bol}}$ vs. $\log_{10} v_{\text{ph}}$	0.67	0.07	0.77	0.03	-	8
$\log_{10} E_K$ vs. $\log_{10} v_{\text{ph}}$	0.25	0.35	0.23	0.4	-	16	$\log_{10} M_{\text{ej}}$ vs. $\log_{10} v_{\text{ph}}$	0.04	0.87	0.06	0.83	-	16
$\log_{10} M_{\text{Ni}}$ vs. $\log_{10} v_{\text{ph}}$	-0.59	0.01	-0.51	0.04	-	17	$\log_{10} T_{90}^*$ vs. k_{avg}	0.24	0.16	0.16	0.36	-	35
$\log_{10} E_{\gamma,\text{iso}}$ vs. k_{avg}	0.24	0.17	0.12	0.5	-	34	$\log_{10} L_{\text{p,bol}}$ vs. k_{avg}	0.33	0.05	0.21	0.22	-	34
$\log_{10} L_{\gamma,\text{iso}}$ vs. k_{avg}	0.11	0.51	-0.02	0.9	-	35	$\log_{10} E_{\gamma,\text{iso}}$ vs. s_{avg}	0.74	< 0.01	0.77	< 0.01	-	16
$\log_{10} t_p^*$ vs. k_{avg}	0.34	0.22	0.34	0.21	-	15	$\Delta m_{15,\text{bol}}$ vs. k_{avg}	-0.19	0.62	-0.18	0.65	-	9
$\log_{10} E_K$ vs. k_{avg}	0.33	0.1	0.34	0.09	-	26	$\log_{10} M_{\text{ej}}$ vs. k_{avg}	0.25	0.22	0.28	0.17	-	26
$\log_{10} M_{\text{Ni}}$ vs. k_{avg}	0.86	< 0.01	0.89	< 0.01	-	30	$\log_{10} v_{\text{ph}}$ vs. k_{avg}	-0.36	0.21	-0.31	0.28	-	14
$\log_{10} T_{90}^*$ vs. s_{avg}	-0.06	0.73	0.0	0.98	-	35	$\log_{10} E_{\gamma,\text{iso}}$ vs. s_{avg}	0.16	0.38	0.21	0.24	-	34
$\log_{10} E_p^*$ vs. s_{avg}	0.15	0.39	0.13	0.47	-	34	$\log_{10} L_{\gamma,\text{iso}}$ vs. s_{avg}	0.23	0.17	0.13	0.44	-	35
$\log_{10} L_{\text{p,bol}}$ vs. s_{avg}	0.21	0.43	0.37	0.16	-	16	$\log_{10} t_p^*$ vs. s_{avg}	0.96	< 0.01	0.9	< 0.01	-	15
$\Delta m_{15,\text{bol}}$ vs. s_{avg}	-0.51	0.17	-0.63	0.07	-	9	$\log_{10} E_K$ vs. s_{avg}	0.81	< 0.01	0.8	< 0.01	-	26

Table 5 continued on next page

Table 5 (*continued*)

Relation	r	P_P	ρ	P_ρ	Notes	N. of points	Relation	r	P_P	ρ	P_ρ	Notes	N. of points
$\log_{10} M_{\text{ej}}$ vs. s_{avg}	0.83	< 0.01	0.83	< 0.01	-	26	$\log_{10} M_{\text{Ni}}$ vs. s_{avg}	0.47	0.01	0.5	< 0.01	-	30
$\log_{10} v_{\text{ph}}$ vs. s_{avg}	-0.49	0.08	-0.48	0.09	-	14	k_{avg} vs. s_{avg}	0.12	0.48	0.24	0.17	3	35
$\log_{10} T_{90}^*$ vs. $\log_{10} T_{\text{a,opt}}^*$	0.4	0.08	0.27	0.25	-	20	$\log_{10} E_{\gamma,\text{iso}}$ vs. $\log_{10} T_{\text{a,opt}}^*$	-0.04	0.88	-0.05	0.84	-	19
$\log_{10} E_p^*$ vs. $\log_{10} T_{\text{a,opt}}^*$	-0.31	0.2	-0.34	0.15	-	19	$\log_{10} L_{\gamma,\text{iso}}$ vs. $\log_{10} T_{\text{a,opt}}^*$	-0.61	< 0.01	-0.27	0.24	1	20
$\log_{10} L_{\text{p,bol}}$ vs. $\log_{10} T_{\text{a,opt}}^*$	-0.28	0.47	-0.38	0.31	-	9	$\log_{10} t_p^*$ vs. $\log_{10} T_{\text{a,opt}}^*$	-0.53	0.14	-0.12	0.77	-	9
$\Delta m_{15,\text{bol}}$ vs. $\log_{10} T_{\text{a,opt}}^*$	0.07	0.9	-0.14	0.79	-	6	$\log_{10} E_K$ vs. $\log_{10} T_{\text{a,opt}}^*$	0.13	0.64	0.32	0.25	-	15
$\log_{10} M_{\text{ej}}$ vs. $\log_{10} T_{\text{a,opt}}^*$	0.11	0.7	0.33	0.24	-	15	$\log_{10} M_{\text{Ni}}$ vs. $\log_{10} T_{\text{a,opt}}^*$	-0.12	0.65	0.25	0.35	-	16
$\log_{10} v_{\text{ph}}$ vs. $\log_{10} T_{\text{a,opt}}^*$	0.29	0.49	0.12	0.78	-	8	k_{avg} vs. $\log_{10} T_{\text{a,opt}}^*$	0.06	0.83	0.17	0.53	-	17
s_{avg} vs. $\log_{10} T_{\text{a,opt}}^*$	-0.28	0.28	0.07	0.8	-	17	$\log_{10} T_{90}$ vs. $\log_{10} T_{\text{a,opt}}^*$	-0.28	0.24	0.0	0.99	-	20
$\log_{10} E_{\gamma,\text{iso}}$ vs. $\log_{10} L_{\text{a,opt}}$	0.41	0.08	0.52	0.02	1	19	$\log_{10} E_p^*$ vs. $\log_{10} L_{\text{a,opt}}$	0.5	0.03	0.54	0.02	1	19
$\log_{10} L_{\gamma,\text{iso}}$ vs. $\log_{10} L_{\text{a,opt}}$	0.74	< 0.01	0.44	0.05	1	20	$\log_{10} L_{\text{p,bol}}$ vs. $\log_{10} L_{\text{a,opt}}$	0.33	0.39	0.3	0.43	-	9
$\log_{10} t_p^*$ vs. $\log_{10} L_{\text{a,opt}}$	0.7	0.04	0.33	0.38	*	9	$\Delta m_{15,\text{bol}}$ vs. $\log_{10} L_{\text{a,opt}}$	-0.29	0.58	-0.14	0.79	-	6
$\log_{10} E_K$ vs. $\log_{10} L_{\text{a,opt}}$	0.01	0.96	0.0	0.99	-	15	$\log_{10} M_{\text{ej}}$ vs. $\log_{10} L_{\text{a,opt}}$	0.03	0.91	0.01	0.97	-	15
$\log_{10} M_{\text{Ni}}$ vs. $\log_{10} L_{\text{a,opt}}$	0.15	0.57	-0.27	0.31	-	16	$\log_{10} v_{\text{ph}}$ vs. $\log_{10} L_{\text{a,opt}}$	-0.19	0.65	-0.07	0.87	-	8
k_{avg} vs. $\log_{10} L_{\text{a,opt}}$	0.06	0.81	-0.2	0.45	-	17	s_{avg} vs. $\log_{10} L_{\text{a,opt}}$	0.31	0.23	0.18	0.5	-	17
$\log_{10} T_{\text{a,opt}}$ vs. $\log_{10} L_{\text{a,opt}}$	-0.8	< 0.01	-0.68	< 0.01	8	20	$\log_{10} T_{90}$ vs. $\log_{10} T_{\text{a,X}}$	0.02	0.96	0.01	0.97	-	14
$\log_{10} E_{\gamma,\text{iso}}$ vs. $\log_{10} L_{\text{a,X}}$	-0.05	0.85	-0.09	0.77	-	14	$\log_{10} E_p^*$ vs. $\log_{10} T_{\text{a,X}}$	0.19	0.54	0.11	0.72	-	13
$\log_{10} L_{\gamma,\text{iso}}$ vs. $\log_{10} T_{\text{a,X}}$	-0.11	0.72	-0.35	0.21	-	14	$\log_{10} L_{\text{p,bol}}$ vs. $\log_{10} T_{\text{a,X}}$	0.53	0.22	0.68	0.09	-	7
$\log_{10} t_p^*$ vs. $\log_{10} T_{\text{a,X}}$	0.18	0.7	0.04	0.94	-	7	$\Delta m_{15,\text{bol}}$ vs. $\log_{10} T_{\text{a,X}}$	-0.05	0.95	0.4	0.6	-	4
$\log_{10} E_K$ vs. $\log_{10} T_{\text{a,X}}$	-0.1	0.78	0.14	0.69	-	11	$\log_{10} M_{\text{ej}}$ vs. $\log_{10} T_{\text{a,X}}$	0.0	0.99	0.18	0.6	-	11
$\log_{10} M_{\text{Ni}}$ vs. $\log_{10} T_{\text{a,X}}$	0.37	0.24	0.39	0.21	-	12	$\log_{10} v_{\text{ph}}$ vs. $\log_{10} T_{\text{a,X}}$	-0.04	0.95	-0.1	0.87	-	5
k_{avg} vs. $\log_{10} T_{\text{a,X}}$	0.46	0.13	0.55	0.06	-	12	s_{avg} vs. $\log_{10} T_{\text{a,X}}$	-0.13	0.69	0.15	0.63	-	12
$\log_{10} T_{\text{a,opt}}$ vs. $\log_{10} T_{\text{a,X}}$	0.31	0.32	0.24	0.44	-	12	$\log_{10} L_{\text{a,opt}}$ vs. $\log_{10} T_{\text{a,X}}$	0.03	0.94	-0.07	0.83	-	12
$\log_{10} T_{90}$ vs. $\log_{10} L_{\text{a,X}}$	0.48	0.08	0.37	0.19	-	14	$\log_{10} E_{\gamma,\text{iso}}$ vs. $\log_{10} L_{\text{a,X}}$	0.56	0.04	0.57	0.03	1	14
$\log_{10} E_p^*$ vs. $\log_{10} L_{\text{a,X}}$	0.2	0.51	0.24	0.43	-	13	$\log_{10} L_{\gamma,\text{iso}}$ vs. $\log_{10} L_{\text{a,X}}$	0.28	0.33	0.42	0.14	-	14
$\log_{10} L_{\text{p,bol}}$ vs. $\log_{10} L_{\text{a,X}}$	-0.02	0.97	0.14	0.76	-	7	$\log_{10} t_p^*$ vs. $\log_{10} L_{\text{a,X}}$	0.16	0.73	0.43	0.34	-	7
$\Delta m_{15,\text{bol}}$ vs. $\log_{10} L_{\text{a,X}}$	-0.1	0.9	0.0	1.0	-	4	$\log_{10} E_K$ vs. $\log_{10} L_{\text{a,X}}$	0.41	0.22	0.37	0.26	-	11
$\log_{10} M_{\text{ej}}$ vs. $\log_{10} L_{\text{a,X}}$	0.24	0.48	0.21	0.54	-	11	$\log_{10} M_{\text{Ni}}$ vs. $\log_{10} L_{\text{a,X}}$	-0.04	0.9	-0.04	0.9	-	12
$\log_{10} v_{\text{ph}}$ vs. $\log_{10} L_{\text{a,X}}$	0.08	0.9	0.3	0.62	-	5	k_{avg} vs. $\log_{10} L_{\text{a,X}}$	-0.05	0.87	-0.18	0.57	-	12
s_{avg} vs. $\log_{10} L_{\text{a,X}}$	0.34	0.28	0.42	0.17	-	12	$\log_{10} T_{\text{a,opt}}$ vs. $\log_{10} L_{\text{a,X}}$	-0.04	0.9	0.04	0.9	-	12
$\log_{10} L_{\text{a,opt}}$ vs. $\log_{10} L_{\text{a,X}}$	0.3	0.35	0.34	0.28	-	12	$\log_{10} T_{\text{a,X}}$ vs. $\log_{10} L_{\text{a,X}}$	-0.74	< 0.01	-0.69	0.01	1	14
$\log_{10} T_{90}$ vs. $\log_{10} \theta_{\text{jet}}$	0.05	0.86	0.02	0.95	-	14	$\log_{10} M_{\text{Ni}}$ vs. $\log_{10} \theta_{\text{jet}}$	0.07	0.8	0.16	0.59	-	14
$\log_{10} E_p^*$ vs. $\log_{10} \theta_{\text{jet}}$	-0.01	0.98	0.01	0.96	-	16	$\log_{10} L_{\gamma,\text{iso}}$ vs. $\log_{10} \theta_{\text{jet}}$	-0.41	0.1	-0.44	0.08	-	17
$\log_{10} L_{\text{p,bol}}$ vs. $\log_{10} \theta_{\text{jet}}$	-0.39	0.34	-0.19	0.65	-	8	$\log_{10} t_p^*$ vs. $\log_{10} \theta_{\text{jet}}$	0.13	0.78	-0.04	0.94	-	7
$\Delta m_{15,\text{bol}}$ vs. $\log_{10} \theta_{\text{jet}}$	0.26	0.58	0.4	0.38	-	7	$\log_{10} E_K$ vs. $\log_{10} \theta_{\text{jet}}$	0.02	0.95	-0.05	0.86	-	14
$\log_{10} M_{\text{ej}}$ vs. $\log_{10} \theta_{\text{jet}}$	-0.19	0.51	-0.19	0.51	-	14	$\log_{10} M_{\text{Ni}}$ vs. $\log_{10} \theta_{\text{jet}}$	0.07	0.8	0.16	0.59	-	14
$\log_{10} E_p^*$ vs. $\log_{10} \theta_{\text{jet}}$	0.74	0.04	0.69	0.06	X	8	k_{avg} vs. $\log_{10} \theta_{\text{jet}}$	0.14	0.64	0.2	0.48	-	14
s_{avg} vs. $\log_{10} \theta_{\text{jet}}$	-0.31	0.29	-0.11	0.71	-	14	$\log_{10} T_{\text{a,opt}}$ vs. $\log_{10} \theta_{\text{jet}}$	0.47	0.29	0.54	0.22	-	7
$\log_{10} L_{\text{a,opt}}$ vs. $\log_{10} \theta_{\text{jet}}$	-0.55	0.2	-0.32	0.48	-	7	$\log_{10} T_{\text{a,X}}$ vs. $\log_{10} \theta_{\text{jet}}$	0.58	0.3	0.9	0.04	-	5

Table 5 continued on next page

Table 5 (continued)

Relation	r	P_P	ρ	P_ρ	Notes	N. of points	Relation	r	P_P	ρ	P_ρ	Notes	N. of points
$\log_{10} L_{a,X}^*$ vs. $\log_{10} \theta_{\text{jet}}$	-0.74	0.15	-0.7	0.19	-	5	$\log_{10} T_{90}^*$ vs. $\log_{10} T_{\text{jet}}^*$	0.03	0.91	-0.03	0.91	-	20
$\log_{10} E_{\gamma,\text{iso}}$ vs. $\log_{10} T_{\text{jet}}^*$	-0.14	0.56	-0.18	0.45	-	20	$\log_{10} E_{\text{p}}^*$ vs. $\log_{10} T_{\text{jet}}^*$	-0.52	0.02	-0.54	0.02	-	19
$\log_{10} L_{\gamma,\text{iso}}$ vs. $\log_{10} T_{\text{jet}}^*$	-0.19	0.42	-0.37	0.11	-	20	$\log_{10} L_{\text{p,bol}}$ vs. $\log_{10} T_{\text{jet}}^*$	-0.32	0.6	-0.3	0.62	-	5
$\log_{10} t_{\text{p}}^*$ vs. $\log_{10} T_{\text{jet}}^*$	-0.21	0.74	-0.7	0.19	-	5	$\Delta m_{15,\text{bol}}$ vs. $\log_{10} T_{\text{jet}}^*$	0.81	0.39	1.0	< 0.01	\times	3
$\log_{10} E_K$ vs. $\log_{10} T_{\text{jet}}^*$	0.08	0.82	0.27	0.42	-	11	$\log_{10} M_{\text{ej}}$ vs. $\log_{10} T_{\text{jet}}^*$	-0.21	0.53	-0.1	0.77	-	11
$\log_{10} M_{\text{Ni}}$ vs. $\log_{10} T_{\text{jet}}^*$	-0.24	0.44	-0.11	0.74	-	12	$\log_{10} v_{\text{ph}}$ vs. $\log_{10} T_{\text{jet}}^*$	-0.44	0.46	-0.3	0.62	-	5
k_{avg} vs. $\log_{10} T_{\text{jet}}^*$	-0.3	0.34	-0.27	0.39	-	12	s_{avg} vs. $\log_{10} T_{\text{jet}}^*$	0.13	0.68	0.21	0.51	-	12
$\log_{10} T_{\text{a,opt}}^*$ vs. $\log_{10} T_{\text{jet}}^*$	0.66	0.1	0.71	0.07	-	7	$\log_{10} L_{\text{a,opt}}$ vs. $\log_{10} T_{\text{jet}}^*$	-0.36	0.43	-0.43	0.34	-	7
$\log_{10} T_{\text{a,X}}^*$ vs. $\log_{10} T_{\text{jet}}^*$	-0.38	0.53	-0.3	0.62	-	5	$\log_{10} L_{\text{a,X}}$ vs. $\log_{10} T_{\text{jet}}^*$	0.39	0.52	0.1	0.87	-	5
$\log_{10} \theta_{\text{jet}}$ vs. $\log_{10} T_{\text{jet}}^*$	0.42	0.26	0.47	0.21	-	9							

NOTE—The legend of the notes is the following: 1) the relation is from Dainotti et al. (2008); 2) the relation is from Amati et al. (2002); 3) the relation is from Cano (2013); 4) the relation is from Yonetoku et al. (2004); 5) the relation is discussed in Shahmoradi & Nemiroff (2015); 6) the relation is from Lü et al. (2018); 7) the relation is from Li (2006b); 8) the relation is from Dainotti et al. (2020b); *) the relation has been found in the current work; \times) this correlation is not investigated due to the paucity of data (less than 5 data points) or the absence of the EP-correction coefficient for one of the two variables. Since in the current Table and in Table 6 the p-value = 0.0 comes from the precision we choose (which is on the second significant digit), all those p-values smaller than this threshold are indicated with are indeed smaller < 0.01 .

Table 6. The cross-relation of GRB and SN observables in the case with the EP correction.

Relation	r	P _P	ρ	P _ρ	P _P	ρ	P _P	ρ	P _ρ	P _P	r	P _P	ρ	P _ρ
$\log_{10} T_{90}^{*'} \text{ vs. } \log_{10} E'_{\gamma,\text{iso}}$	0.41	< 0.01	0.42	< 0.01	$\log_{10} T_{90}^{*'} \text{ vs. } \log_{10} E'_{\gamma,\text{iso}}$	0.33	0.02	0.35	0.01	$\log_{10} E'_{\gamma,\text{iso}} \text{ vs. } \log_{10} E'_{\gamma,\text{iso}}$	0.65	< 0.01	0.65	< 0.01
$\log_{10} T_{90}^{*'} \text{ vs. } \log_{10} L'_{\gamma,\text{iso}}$	-0.33	0.01	-0.23	0.09	$\log_{10} E'_{\gamma,\text{iso}} \text{ vs. } \log_{10} L'_{\gamma,\text{iso}}$	0.76	< 0.01	0.74	< 0.01	$\log_{10} E'_{\gamma,\text{iso}} \text{ vs. } \log_{10} L'_{\gamma,\text{iso}}$	0.44	< 0.01	0.49	< 0.01
$\log_{10} T_{90}^{*'} \text{ vs. } \log_{10} L'_{\text{p,bol}}$	0.26	0.31	0.21	0.42	$\log_{10} E'_{\gamma,\text{iso}} \text{ vs. } \log_{10} L'_{\text{p,bol}}$	0.24	0.38	0.22	0.42	$\log_{10} E'_{\gamma,\text{iso}} \text{ vs. } \log_{10} L'_{\text{p,bol}}$	0.36	0.17	0.38	0.15
$\log_{10} L'_{\gamma,\text{iso}} \text{ vs. } \log_{10} L'_{\text{p,bol}}$	0.0	0.99	-0.05	0.86	$\log_{10} T_{90}^{*'} \text{ vs. } \log_{10} t_{\text{p}}^{*'}$	-0.12	0.66	-0.09	0.75	$\log_{10} E'_{\gamma,\text{iso}} \text{ vs. } \log_{10} t_{\text{p}}^{*'}$	0.18	0.54	0.07	0.82
$\log_{10} L'_{\text{p}} \text{ vs. } \log_{10} t_{\text{p}}^{*'}$	0.17	0.54	0.32	0.25	$\log_{10} L'_{\gamma,\text{iso}} \text{ vs. } \log_{10} t_{\text{p}}^{*'}$	0.35	0.2	0.1	0.73	$\log_{10} L'_{\text{p,bol}} \text{ vs. } \log_{10} t_{\text{p}}^{*'}$	0.12	0.66	0.21	0.44
$\log_{10} T_{90}^{*'} \text{ vs. } \Delta m_{15,\text{bol}}$	0.48	0.2	0.64	0.07	$\log_{10} E'_{\gamma,\text{iso}} \text{ vs. } \Delta m_{15,\text{bol}}$	-0.04	0.92	-0.04	0.93	$\log_{10} E'_{\gamma,\text{iso}} \text{ vs. } \Delta m_{15,\text{bol}}$	-0.16	0.7	-0.36	0.39
$\log_{10} L'_{\gamma,\text{iso}} \text{ vs. } \Delta m_{15,\text{bol}}$	-0.46	0.21	-0.43	0.25	$\log_{10} L'_{\text{p,bol}} \text{ vs. } \Delta m_{15,\text{bol}}$	-0.18	0.65	-0.24	0.53	$\log_{10} t_{\text{p}}^{*'} \text{ vs. } \Delta m_{15,\text{bol}}$	-0.58	0.1	-0.59	0.1
$\log_{10} T_{90}^{*'} \text{ vs. } \log_{10} E'_{\text{K}}$	0.09	0.65	-0.08	0.69	$\log_{10} E'_{\gamma,\text{iso}} \text{ vs. } \log_{10} E'_{\text{K}}$	-0.03	0.87	0.08	0.69	$\log_{10} E'_{\text{p}} \text{ vs. } \log_{10} E'_{\text{K}}$	0.09	0.64	0.08	0.69
$\log_{10} L'_{\gamma,\text{iso}} \text{ vs. } \log_{10} E'_{\text{K}}$	-0.01	0.97	0.0	0.98	$\log_{10} L'_{\text{p,bol}} \text{ vs. } \log_{10} E'_{\text{K}}$	-0.13	0.67	-0.04	0.9	$\log_{10} t_{\text{p}}^{*'} \text{ vs. } \log_{10} E'_{\text{K}}$	0.22	0.49	0.32	0.31
$\Delta m_{15,\text{bol}} \text{ vs. } \log_{10} E'_{\text{K}}$	-0.41	0.28	-0.49	0.18	$\log_{10} T_{90}^{*'} \text{ vs. } \log_{10} M_{\text{ej}}$	-0.13	0.5	-0.15	0.43	$\log_{10} E'_{\gamma,\text{iso}} \text{ vs. } \log_{10} M_{\text{ej}}$	-0.05	0.8	0.01	0.96
$\log_{10} E'_{\text{p}} \text{ vs. } \log_{10} M_{\text{ej}}$	0.08	0.68	0.03	0.88	$\log_{10} L'_{\gamma,\text{iso}} \text{ vs. } \log_{10} M_{\text{ej}}$	0.09	0.66	0.08	0.68	$\log_{10} L'_{\text{p,bol}} \text{ vs. } \log_{10} M_{\text{ej}}$	0.03	0.92	-0.07	0.81
$\log_{10} t_{\text{p}}^{*'} \text{ vs. } \log_{10} M_{\text{ej}}$	0.32	0.3	0.22	0.5	$\Delta m_{15,\text{bol}} \text{ vs. } \log_{10} M_{\text{ej}}$	-0.73	0.02	-0.7	0.04	$\log_{10} E'_{\text{p}} \text{ vs. } \log_{10} M_{\text{ej}}$	0.73	< 0.01	0.81	< 0.01
$\log_{10} T_{90}^{*'} \text{ vs. } \log_{10} M_{\text{Ni}}$	0.13	0.48	0.07	0.7	$\log_{10} E'_{\gamma,\text{iso}} \text{ vs. } \log_{10} M_{\text{Ni}}$	0.29	0.11	0.25	0.17	$\log_{10} E'_{\text{p}} \text{ vs. } \log_{10} M_{\text{Ni}}$	0.34	0.05	0.34	0.05
$\log_{10} L'_{\gamma,\text{iso}} \text{ vs. } \log_{10} M_{\text{Ni}}$	0.2	0.27	0.14	0.44	$\log_{10} L'_{\text{p,bol}} \text{ vs. } \log_{10} M_{\text{Ni}}$	0.68	< 0.01	0.83	< 0.01	$\log_{10} t_{\text{p}}^{*'} \text{ vs. } \log_{10} M_{\text{Ni}}$	0.34	0.2	0.31	0.25
$\Delta m_{15,\text{bol}} \text{ vs. } \log_{10} M_{\text{Ni}}$	-0.25	0.51	-0.36	0.34	$\log_{10} E'_{\text{K}} \text{ vs. } \log_{10} M_{\text{Ni}}$	0.34	0.05	0.34	0.06	$\log_{10} M_{\text{ej}} \text{ vs. } \log_{10} M_{\text{Ni}}$	0.26	0.15	0.27	0.13
$\log_{10} T_{90}^{*'} \text{ vs. } \log_{10} v_{\text{ph}}$	0.34	0.17	0.42	0.08	$\log_{10} E'_{\gamma,\text{iso}} \text{ vs. } \log_{10} v_{\text{ph}}$	-0.18	0.51	-0.23	0.4	$\log_{10} E'_{\text{p}} \text{ vs. } \log_{10} v_{\text{ph}}$	-0.23	0.39	-0.23	0.4
$\log_{10} L'_{\gamma,\text{iso}} \text{ vs. } \log_{10} v_{\text{ph}}$	-0.41	0.12	-0.49	0.05	$\log_{10} L'_{\text{p,bol}} \text{ vs. } \log_{10} v_{\text{ph}}$	-0.13	0.68	-0.29	0.34	$\log_{10} t_{\text{p}}^{*'} \text{ vs. } \log_{10} v_{\text{ph}}$	-0.45	0.14	-0.36	0.25
$\Delta m_{15,\text{bol}} \text{ vs. } \log_{10} v_{\text{ph}}$	0.67	0.07	0.77	0.03	$\log_{10} E'_{\text{K}} \text{ vs. } \log_{10} v_{\text{ph}}$	0.25	0.36	0.19	0.48	$\log_{10} M_{\text{ej}} \text{ vs. } \log_{10} v_{\text{ph}}$	0.04	0.87	0.06	0.83
$\log_{10} M_{\text{Ni}} \text{ vs. } \log_{10} v_{\text{ph}}$	-0.59	0.01	-0.51	0.04	$\log_{10} T_{90}^{*'} \text{ vs. } k_{\text{avg}}$	0.25	0.15	0.16	0.35	$\log_{10} E'_{\gamma,\text{iso}} \text{ vs. } k_{\text{avg}}$	0.27	0.13	0.13	0.46
$\log_{10} E'_{\text{p}} \text{ vs. } k_{\text{avg}}$	0.34	0.05	0.26	0.14	$\log_{10} L'_{\gamma,\text{iso}} \text{ vs. } k_{\text{avg}}$	0.12	0.48	0.04	0.8	$\log_{10} L'_{\text{p,bol}} \text{ vs. } k_{\text{avg}}$	0.74	< 0.01	0.76	< 0.01
$\log_{10} t_{\text{p}}^{*'} \text{ vs. } k_{\text{avg}}$	0.26	0.35	0.19	0.51	$\Delta m_{15,\text{bol}} \text{ vs. } k_{\text{avg}}$	-0.19	0.62	-0.18	0.65	$\log_{10} E'_{\text{K}} \text{ vs. } k_{\text{avg}}$	0.33	0.1	0.33	0.1
$\log_{10} M_{\text{ej}} \text{ vs. } k_{\text{avg}}$	0.25	0.22	0.28	0.17	$\log_{10} M_{\text{Ni}} \text{ vs. } k_{\text{avg}}$	0.86	< 0.01	0.89	< 0.01	$\log_{10} v_{\text{ph}} \text{ vs. } k_{\text{avg}}$	-0.36	0.21	-0.31	0.28
$\log_{10} T_{90}^{*'} \text{ vs. } s_{\text{avg}}$	-0.05	0.77	-0.04	0.82	$\log_{10} E'_{\gamma,\text{iso}} \text{ vs. } s_{\text{avg}}$	0.05	0.76	0.14	0.44	$\log_{10} E'_{\text{p}} \text{ vs. } s_{\text{avg}}$	0.08	0.64	0.04	0.81
$\log_{10} L'_{\gamma,\text{iso}} \text{ vs. } s_{\text{avg}}$	0.13	0.45	0.06	0.74	$\log_{10} L'_{\text{p,bol}} \text{ vs. } s_{\text{avg}}$	0.18	0.5	0.25	0.34	$\log_{10} t_{\text{p}}^{*'} \text{ vs. } s_{\text{avg}}$	0.88	< 0.01	0.68	0.01
$\Delta m_{15,\text{bol}} \text{ vs. } s_{\text{avg}}$	-0.51	0.16	-0.56	0.12	$\log_{10} E'_{\text{K}} \text{ vs. } s_{\text{avg}}$	0.82	< 0.01	0.8	< 0.01	$\log_{10} M_{\text{ej}} \text{ vs. } s_{\text{avg}}$	0.85	< 0.01	0.84	< 0.01
$\log_{10} M_{\text{Ni}} \text{ vs. } s_{\text{avg}}$	0.48	0.01	0.5	0.01	$\log_{10} v_{\text{ph}} \text{ vs. } s_{\text{avg}}$	-0.49	0.08	-0.49	0.08	$k_{\text{avg}} \text{ vs. } s_{\text{avg}}$	0.13	0.46	0.21	0.22
$\log_{10} T_{90}^{*'} \text{ vs. } \log_{10} T_{\text{a,opt}}$	0.39	0.09	0.32	0.17	$\log_{10} E'_{\gamma,\text{iso}} \text{ vs. } \log_{10} T_{\text{a,opt}}$	0.07	0.79	0.15	0.53	$\log_{10} E'_{\text{p}} \text{ vs. } \log_{10} T_{\text{a,opt}}$	-0.2	0.41	-0.23	0.35
$\log_{10} L'_{\gamma,\text{iso}} \text{ vs. } \log_{10} T_{\text{a,opt}}$	-0.52	0.02	-0.27	0.26	$\log_{10} L'_{\text{p,bol}} \text{ vs. } \log_{10} T_{\text{a,opt}}$	-0.14	0.71	0.07	0.86	$\log_{10} t_{\text{p}}^{*'} \text{ vs. } \log_{10} T_{\text{a,opt}}$	-0.6	0.09	-0.57	0.11
$\Delta m_{15,\text{bol}} \text{ vs. } T_{\text{a,opt}}$	0.05	0.93	-0.03	0.36	$\log_{10} E'_{\text{K}} \text{ vs. } \log_{10} T_{\text{a,opt}}$	0.16	0.56	0.34	0.22	$\log_{10} M_{\text{ej}} \text{ vs. } \log_{10} T_{\text{a,opt}}$	0.14	0.63	0.29	0.3
$\log_{10} M_{\text{Ni}} \text{ vs. } \log_{10} T_{\text{a,opt}}$	-0.1	0.73	0.24	0.36	$\log_{10} v_{\text{ph}} \text{ vs. } \log_{10} T_{\text{a,opt}}$	0.22	0.6	0.17	0.69	$k_{\text{avg}} \text{ vs. } \log_{10} T_{\text{a,opt}}$	0.05	0.84	0.12	0.65
$s_{\text{avg}} \text{ vs. } \log_{10} T_{\text{a,opt}}$	-0.19	0.47	0.1	0.71	$\log_{10} T_{90}^{*'} \text{ vs. } \log_{10} L'_{\text{a,opt}}$	-0.24	0.31	0.05	0.84	$\log_{10} E'_{\gamma,\text{iso}} \text{ vs. } \log_{10} L'_{\text{a,opt}}$	0.4	0.09	0.54	0.02
$\log_{10} E'_{\text{p}} \text{ vs. } \log_{10} L'_{\text{a,opt}}$	0.45	0.06	0.59	0.01	$\log_{10} L'_{\gamma,\text{iso}} \text{ vs. } \log_{10} L'_{\text{a,opt}}$	0.7	< 0.01	0.43	0.06	$\log_{10} L'_{\text{p,bol}} \text{ vs. } \log_{10} L'_{\text{a,opt}}$	0.23	0.54	0.07	0.86
$\log_{10} t_{\text{p}}^{*'} \text{ vs. } \log_{10} L'_{\text{a,opt}}$	0.71	0.03	0.27	0.49	$\Delta m_{15,\text{bol}} \text{ vs. } \log_{10} L'_{\text{a,opt}}$	-0.32	0.53	0.03	0.96	$\log_{10} E'_{\text{K}} \text{ vs. } \log_{10} L'_{\text{a,opt}}$	-0.02	0.93	-0.02	0.94
$\log_{10} M_{\text{ej}} \text{ vs. } \log_{10} L'_{\text{a,opt}}$	0.01	0.96	0.05	0.85	$\log_{10} M_{\text{Ni}} \text{ vs. } \log_{10} L'_{\text{a,opt}}$	0.11	0.69	-0.27	0.32	$\log_{10} v_{\text{ph}} \text{ vs. } \log_{10} L'_{\text{a,opt}}$	-0.08	0.86	0.17	0.69
$k_{\text{avg}} \text{ vs. } \log_{10} L'_{\text{a,opt}}$	0.08	0.75	-0.08	0.76	$s_{\text{avg}} \text{ vs. } \log_{10} L'_{\text{a,opt}}$	0.2	0.44	0.07	0.79	$\log_{10} T_{\text{a,opt}} \text{ vs. } \log_{10} L'_{\text{a,opt}}$	-0.7	< 0.01	-0.57	0.01
$\log_{10} T_{90}^{*'} \text{ vs. } \log_{10} T_{\text{a,X}}$	0.04	0.9	0.13	0.66	$\log_{10} E'_{\gamma,\text{iso}} \text{ vs. } \log_{10} T_{\text{a,X}}$	-0.04	0.88	-0.02	0.93	$\log_{10} E'_{\text{p}} \text{ vs. } \log_{10} T_{\text{a,X}}$	0.18	0.56	0.11	0.72
$\log_{10} L'_{\gamma,\text{iso}} \text{ vs. } \log_{10} T_{\text{a,X}}$	-0.13	0.67	-0.31	0.27	$\log_{10} L'_{\text{p,bol}} \text{ vs. } \log_{10} T_{\text{a,X}}$	0.58	0.17	0.71	0.07	$\log_{10} t_{\text{p}}^{*'} \text{ vs. } \log_{10} T_{\text{a,X}}$	0.12	0.8	0.29	0.53

Table 6 continued on next page

Table 6 (continued)

Relation	r	P _P	ρ	P _p	Relation	r	P _P	ρ	P _p	Relation	r	P _P	ρ	P _p
$\Delta m_{15,\text{bol}}$ vs. $\log_{10} T_{\text{a},X}^{*'}$	-0.01	0.99	0.4	0.6	$\log_{10} E'_{\text{K}}$ vs. $\log_{10} T_{\text{a},X}^{*'}$	-0.1	0.76	0.12	0.73	$\log_{10} M_{\text{ej}}$ vs. $\log_{10} T_{\text{a},X}^{*'}$	-0.01	0.97	0.18	0.6
$\log_{10} M_{\text{Ni}}$ vs. $\log_{10} T_{\text{a},X}^{*'}$	0.37	0.24	0.4	0.2	$\log_{10} v_{\text{ph}}$ vs. $\log_{10} T_{\text{a},X}^{*'}$	-0.04	0.94	-0.1	0.87	k_{avg} vs. $\log_{10} T_{\text{a},X}^{*'}$	0.48	0.12	0.57	0.05
s_{avg} vs. $\log_{10} T_{\text{a},X}^{*'}$	-0.14	0.66	0.09	0.78	$\log_{10} T_{\text{a},\text{opt}}^{*'}$ vs. $\log_{10} T_{\text{a},X}^{*'}$	0.35	0.26	0.3	0.34	$\log_{10} L'_{\text{a},\text{opt}}$ vs. $\log_{10} T_{\text{a},X}^{*'}$	-0.03	0.93	-0.13	0.68
$\log_{10} T_{\gamma}^{*}$ vs. $\log_{10} L_{\text{a},X}^{*'}$	0.45	0.1	0.26	0.37	$\log_{10} E'_{\gamma,\text{iso}}$ vs. $\log_{10} L_{\text{a},X}^{*'}$	0.54	0.05	0.55	0.04	$\log_{10} E'_{\text{p}}$ vs. $\log_{10} L_{\text{a},X}^{*'}$	0.19	0.54	0.27	0.37
$\log_{10} L'_{\gamma,\text{iso}}$ vs. $\log_{10} L_{\text{a},X}^{*'}$	0.25	0.4	0.37	0.2	$\log_{10} L'_{\text{p,bol}}$ vs. $\log_{10} L_{\text{a},X}^{*'}$	-0.08	0.86	0.11	0.82	$\log_{10} t_{\text{p}}^{*}$ vs. $\log_{10} L_{\text{a},X}^{*'}$	0.24	0.6	0.36	0.43
$\Delta m_{15,\text{bol}}$ vs. $\log_{10} L_{\text{a},X}^{*'}$	-0.13	0.87	0.0	1.0	$\log_{10} E'_{\text{K}}$ vs. $\log_{10} L_{\text{a},X}^{*'}$	0.44	0.18	0.39	0.23	$\log_{10} M_{\text{ej}}$ vs. $\log_{10} L_{\text{a},X}^{*'}$	0.27	0.42	0.21	0.54
$\log_{10} M_{\text{Ni}}$ vs. $\log_{10} L_{\text{a},X}^{*'}$	-0.04	0.9	0.01	0.98	$\log_{10} v_{\text{ph}}$ vs. $\log_{10} L_{\text{a},X}^{*'}$	0.09	0.89	0.3	0.62	k_{avg} vs. $\log_{10} L_{\text{a},X}^{*'}$	-0.09	0.78	-0.16	0.62
s_{avg} vs. $\log_{10} L_{\text{a},X}^{*'}$	0.34	0.28	0.48	0.12	$\log_{10} T_{\text{a},\text{opt}}^{*'}$ vs. $\log_{10} L_{\text{a},X}^{*'}$	-0.05	0.87	0.01	0.98	$\log_{10} L'_{\text{a,opt}}$ vs. $\log_{10} L_{\text{a},X}^{*'}$	0.34	0.28	0.36	0.25
$\log_{10} T_{\text{a},X}^{*'}$ vs. $\log_{10} L_{\text{a},X}^{*'}$	-0.75	< 0.01	-0.71	< 0.01	$\log_{10} T_{\text{90}}^{*}$ vs. $\log_{10} \theta'_{\text{jet}}$	0.02	0.95	0.03	0.9	$\log_{10} E'_{\gamma,\text{iso}}$ vs. $\log_{10} \theta'_{\text{jet}}$	-0.54	0.02	-0.54	0.03
$\log_{10} E'_{\text{p}}$ vs. $\log_{10} \theta'_{\text{jet}}$	-0.09	0.73	-0.09	0.75	$\log_{10} L'_{\gamma,\text{iso}}$ vs. $\log_{10} \theta'_{\text{jet}}$	-0.58	0.02	-0.65	< 0.01	$\log_{10} L'_{\text{p,bol}}$ vs. $\log_{10} \theta'_{\text{jet}}$	-0.48	0.23	-0.17	0.69
$\log_{10} t_{\text{p}}^{*}$ vs. $\log_{10} \theta'_{\text{jet}}$	-0.1	0.83	-0.04	0.94	$\Delta m_{15,\text{bol}}$ vs. $\log_{10} \theta'_{\text{jet}}$	0.31	0.5	0.31	0.5	$\log_{10} E'_{\text{K}}$ vs. $\log_{10} \theta'_{\text{jet}}$	0.01	0.98	-0.02	0.93
$\log_{10} M_{\text{ej}}$ vs. $\log_{10} \theta'_{\text{jet}}$	-0.15	0.6	-0.13	0.67	$\log_{10} M_{\text{Ni}}$ vs. $\log_{10} \theta'_{\text{jet}}$	0.07	0.81	0.16	0.58	$\log_{10} v_{\text{ph}}$ vs. $\log_{10} \theta'_{\text{jet}}$	0.72	0.04	0.61	0.11
k_{avg} vs. $\log_{10} \theta'_{\text{jet}}$	0.11	0.71	0.24	0.42	s_{avg} vs. $\log_{10} \theta'_{\text{jet}}$	-0.2	0.49	-0.09	0.77	$\log_{10} T_{\text{a},\text{opt}}^{*'}$ vs. $\log_{10} \theta'_{\text{jet}}$	0.56	0.2	0.54	0.22
$\log_{10} L'_{\text{a},\text{opt}}$ vs. $\log_{10} \theta'_{\text{jet}}$	-0.65	0.11	-0.32	0.48	$\log_{10} T_{\text{a},X}^{*'}$ vs. $\log_{10} \theta'_{\text{jet}}$	0.49	0.4	0.8	0.1	$\log_{10} L'_{\text{a},X}$ vs. $\log_{10} \theta'_{\text{jet}}$	-0.73	0.16	-0.7	0.19
$\log_{10} T_{\text{90}}^{*}$ vs. $\log_{10} T_{\text{jet}}^{*}$	0.01	0.98	-0.06	0.79	$\log_{10} E'_{\gamma,\text{iso}}$ vs. $\log_{10} T_{\text{jet}}^{*}$	-0.09	0.72	-0.16	0.49	$\log_{10} E'_{\text{p}}$ vs. $\log_{10} T_{\text{jet}}^{*}$	-0.53	0.02	-0.54	0.02
$\log_{10} L'_{\gamma,\text{iso}}$ vs. $\log_{10} T_{\text{jet}}^{*}$	-0.09	0.71	-0.3	0.19	$\log_{10} L'_{\text{p,bol}}$ vs. $\log_{10} T_{\text{jet}}^{*}$	-0.4	0.51	-0.1	0.87	$\log_{10} t_{\text{p}}^{*}$ vs. $\log_{10} T_{\text{jet}}^{*}$	0.14	0.82	-0.2	0.75
$\Delta m_{15,\text{bol}}$ vs. $\log_{10} T_{\text{jet}}^{*}$	0.81	0.39	1.0	< 0.01	$\log_{10} E'_{\text{K}}$ vs. $\log_{10} T_{\text{jet}}^{*}$	0.07	0.84	0.27	0.42	$\log_{10} M_{\text{ej}}$ vs. $\log_{10} T_{\text{jet}}^{*}$	-0.21	0.53	-0.1	0.77
$\log_{10} M_{\text{Ni}}$ vs. $\log_{10} T_{\text{jet}}^{*}$	-0.24	0.44	-0.11	0.74	$\log_{10} v_{\text{ph}}$ vs. $\log_{10} T_{\text{jet}}^{*}$	-0.44	0.46	-0.3	0.62	k_{avg} vs. $\log_{10} T_{\text{jet}}^{*}$	-0.3	0.34	-0.27	0.39
s_{avg} vs. $\log_{10} T_{\text{jet}}^{*}$	0.19	0.56	0.28	0.38	$\log_{10} T_{\text{a},\text{opt}}^{*'}$ vs. $\log_{10} T_{\text{jet}}^{*}$	0.72	0.07	0.79	0.04	$\log_{10} L'_{\text{a},\text{opt}}$ vs. $\log_{10} T_{\text{jet}}^{*}$	-0.26	0.57	-0.29	0.53
$\log_{10} T_{\text{a},X}^{*'}$ vs. $\log_{10} T_{\text{jet}}^{*}$	-0.4	0.51	-0.3	0.62	$\log_{10} L'_{\text{a},X}$ vs. $\log_{10} T_{\text{jet}}^{*}$	0.44	0.46	0.1	0.87	$\log_{10} \theta'_{\text{jet}}$ vs. $\log_{10} T_{\text{jet}}^{*}$	0.47	0.2	0.47	0.21

Note.—Since the checked correlations of this table are the same as Table 5, the notes' column and the number of data points will be omitted. See the previous Table 5 for the references.

B. THE ODR METHOD

The ODR method (Boggs & Donaldson 1989) deals with the problem of best fitting for data when the uncertainties are present not only on the dependent variable (x) but also on the independent variables (y) that are present in the correlations.

Let us call (x_i, y_i) , with $i = 1, \dots, N$, the pairs of independent and dependent observed variables, respectively. If we consider (X_i, Y_i) as the true values of the variables and (δ_i, ϵ_i) the random errors associated with x_i and y_i , respectively, we can say that $x_i = X_i - \delta_i$ and $y_i = Y_i - \epsilon_i$. Furthermore, it can be assumed that Y_i is a smooth function of X_i and a set of parameters β , namely $Y_i = f(X_i, \beta)$: this condition can be recast as $y_i = f(x_i + \delta_i, \beta) - \epsilon_i$. An ODR problem is based on the minimization of the orthogonal distance, R_i , from the point (x_i, y_i) to the curve expressed by $f(\hat{x}, \hat{\beta})$ (where the $\hat{\cdot}$ notation denotes a generic choice for the values). If the hypothesis of Gaussian distributions for the errors δ_i and ϵ_i is assumed, then the ODR problem can be written as:

$$R_i^2 = \min_{\hat{\beta}, \hat{\delta}} \sum_{i=1}^N w_i^2 [(f(x_i + \hat{\delta}_i, \hat{\beta}) - y_i)^2 + d_i^2 \hat{\delta}_i^2], \quad (4)$$

where the constraint given by $y_i = f(x_i + \hat{\delta}_i, \hat{\beta}) - \hat{\epsilon}_i$ substituted the $\hat{\epsilon}_i$, $w_i \geq 0$ and $d_i > 0$ are the weights for the problem in the general form. In our case, we consider the following expressions for the weights: $w_i = 1/\sigma_{\epsilon_i}$ and $d_i = \sigma_{\epsilon_i}/\sigma_{\delta_i}$ (Boggs & Donaldson 1989). We here remark that the ODR method corresponds to a fitting with the weights on only one variable when the other variable has no associated uncertainties and, thus, no defined weights.

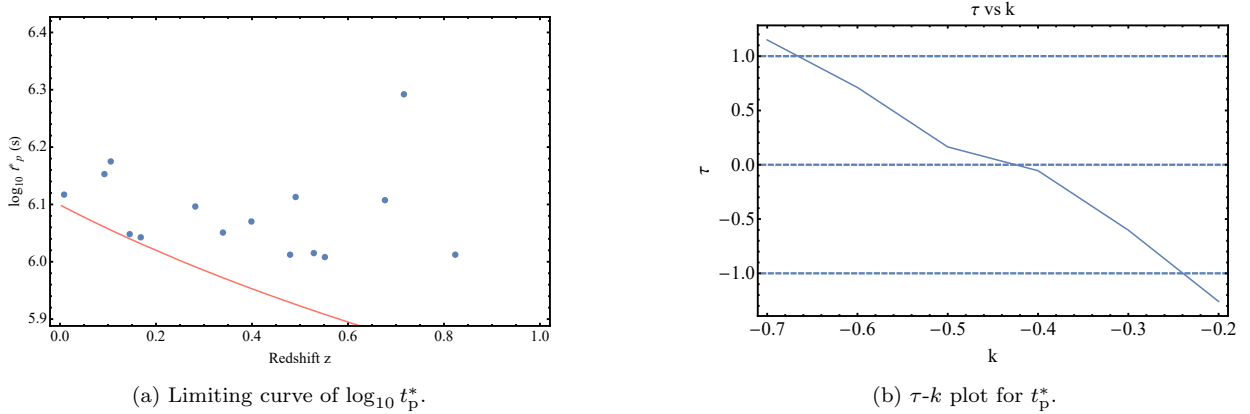


Figure 6. (a) The limiting curve applied to the variable $t_p^{* \prime}$ expressed as the \log_{10} of its values in s. (b) The plot τ - k for this variable: it can be seen that $k_{t_p^{* \prime}}$ value is obtained at the level $\tau = 0$.

C. THE EP METHOD

GRB correlations are affected by biases resulting from sample size and selection effects due to instrumental thresholds (Dainotti et al. 2013, 2015; Dainotti & Del Vecchio 2017; Dainotti et al. 2020a, 2021a, 2022b). To determine whether the GRB-SNe correlations plotted in the scatter matrix are intrinsic or affected by these biases, we utilize the EP method (Efron & Petrosian 1992) to create new corrected and unbiased data, the so-called *local variables*, denoted with the symbol $'$. Previous studies have successfully applied this method to remove biases due to the incomplete data and to remove the cosmological evolution of the variables (Lloyd & Petrosian 2000; Kocevski & Liang 2006; Petrosian et al. 2009; Dainotti et al. 2013, 2015; Dainotti & Del Vecchio 2017; Dainotti & Amati 2018; Dainotti et al. 2020a). The EP method employs a modification of the Kendall τ rank test (Kendall 1948) to determine the dependence of a selected variable, x , on the GRB-SN's redshift, z , namely the *evolution of variable* (see Dainotti et al. (2013) and references therein, i.e. Singal et al. (2011)). The test statistic is defined as

$$\tau = \frac{\sum_i (\mathcal{R}_i - \mathcal{E}_i)}{\sqrt{\sum_i \mathcal{V}_i}}, \quad (5)$$

where \mathcal{R}_i is the rank of the selected variable, x_i , of the i -th data point, (z_i, x_i) , within its *associated set*. For truncated data, the associated set relative to a given data point consists of the points having a lower redshift that would have been observed at the redshift of the given GRB characterized by z_i and L_i and with a luminosity (or energy) higher than the minimum one determined by that given GRB. Thus, for the i -th data point, for luminosity-like and energy-like properties, the associated set for determining the evolution of variable x is:

$$J_i \equiv \{j: z_j < z_{\max}(x_i)\} \cup \{j: x_j > x_i\}, \quad (6)$$

where $z_{\max}(x_i)$ is the maximum redshift at which the i -th object could be placed and still be included in the survey for the given variable. For time-like properties, the associated set is:

$$J_i \equiv \{j: z_j > z_{\min}(x_i)\} \cup \{j: x_j > x_i\}, \quad (7)$$

where $z_{\min}(x_i)$ is the minimum redshift at which the i -th object could be placed and still be included in the survey. If x is not dependent on z , the rank \mathcal{R}_i has then a continuous distribution in the $(0, 1)$ interval, an the expectation value $\mathcal{E}_i = \frac{1}{2}(i+1)$ and variance $\mathcal{V}_i = \frac{1}{12}(i^2+1)$.

The mean and variance are estimated separately for each associated set and summed to find a single value for τ , and independence is rejected at the $n\sigma$ level if $|\tau| > n$.

For a selected variable x , the τ_x test statistic represents the degree of correlation for the truncated sample and is used to find the best-fit parametrization describing the evolution of x and, in particular, the slope of the evolutionary function, k_x . The found value of k_x is then used in a correlation function $g(z)$ to de-evolve the selected variable and thereby determine the local variable, $x' = x/g(z)$. Here, we choose the simple correlation function, $f(z) = (1+z)^k$, since previous investigations tested more complex functions and obtained results compatible with those found using the simple function (Dainotti & Del Vecchio 2017). The local variable is then defined as $x' = x/(1+z)^{k_x}$.

We plot a limiting curve alongside the data based on observational limitations for the variables of interest. For the time, we consider the limiting time as $T^{*\text{lim}} = T_{\text{lim}}/(1+z)$ where T_{lim} is the observed limiting time, see the left panel of Figure 6.

For luminosity and energy properties, we determine the minimum observable value for a given redshift using a limiting flux, F_{lim} , or fluence, f_{lim} , to calculate a limiting luminosity, $L_{\text{lim}} = 4\pi D_L^2(z) F_{\text{lim}}$, or limiting energy, $E_{\text{lim}} = 4\pi D_L^2(z) f_{\text{lim}}$, respectively, where $D_L^2(z)$ is the luminosity distance of a given GRB-SN. The limiting sensitivity of Swift satellite XRT, $F_{\text{lim}} = 10^{-14} \text{ erg cm}^{-2} \text{ s}^{-1}$, is not high enough to describe the truncation of our sample. Seeking a compromise between retaining $\gtrsim 90\%$ of the plotted GRB-SNe and a reasonable estimation of the truncation, we keep on restricting the limiting value until the curve has good agreement with the data. For other reported properties, we begin with the minimum value of the data set, and likewise further restrict the value until the limiting curve is representative of the data. Finally, the Kendall τ is computed for several values of the slope of the evolutionary functions, k , until we find values of k for which $\tau = 0$ with $1-\sigma$ uncertainty given by $|\tau_x| \leq 1$ (see the right panel of Figure 6).

REFERENCES

- Abbott, B. P., Abbott, R., Abbott, T. D., et al. 2017, The Astrophysical Journal, 848, L12, doi: [10.3847/2041-8213/aa91c9](https://doi.org/10.3847/2041-8213/aa91c9)
- Aguilera-Dena, D. R., Langer, N., Moriya, T. J., & Schootemeijer, A. 2018, The Astrophysical Journal, 858, 115, doi: [10.3847/1538-4357/aabfc1](https://doi.org/10.3847/1538-4357/aabfc1)
- Aloy, M. A., Mueller, E., Ibanez, J. M., Marti, J. M., & MacFadyen, A. 1999, Relativistic Jets from Collapsars. <https://arxiv.org/abs/astro-ph/9910466>
- Amati, L. 2008, in The Eleventh Marcel Grossmann Meeting On Recent Developments in Theoretical and Experimental General Relativity, Gravitation and Relativistic Field Theories, 1965–1967, doi: [10.1142/9789812834300_0299](https://doi.org/10.1142/9789812834300_0299)
- Amati, L., Frontera, F., Tavani, M., et al. 2002, Astronomy & Astrophysics, 390, 81–89, doi: [10.1051/0004-6361:20020722](https://doi.org/10.1051/0004-6361:20020722)
- Arnett, W. D. 1982, The Astrophysical Journal, 253, 785, doi: [10.1086/159681](https://doi.org/10.1086/159681)
- Ashall, C., Mazzali, P. A., Pian, E., et al. 2019, Monthly Notices of the Royal Astronomical Society, 487, 5824–5839, doi: [10.1093/mnras/stz1588](https://doi.org/10.1093/mnras/stz1588)
- Barthelmy, S. 2011, GRB 171205A: Swift-BAT refined analysis, NASA. <https://gcn.gsfc.nasa.gov/gcn3/22184.gcn3>
- Bartoli, B., Bernardini, P., Bi, X. J., et al. 2017, The Astrophysical Journal, 842, 31, doi: [10.3847/1538-4357/aa74bc](https://doi.org/10.3847/1538-4357/aa74bc)
- Berger, E., Chornock, R., Holmes, T. R., et al. 2011, The Astrophysical Journal, 743, 204, doi: [10.1088/0004-637X/743/2/204](https://doi.org/10.1088/0004-637X/743/2/204)
- Berger, E., Chornock, R., Holmes, T. R., et al. 2011, The Astrophysical Journal, 743, 204, doi: [10.1088/0004-637X/743/2/204](https://doi.org/10.1088/0004-637X/743/2/204)
- Bianco, F. B., Modjaz, M., Hicken, M., et al. 2014, The Astrophysical Journal Supplement Series, 213, 19, doi: [10.1088/0067-0049/213/2/19](https://doi.org/10.1088/0067-0049/213/2/19)
- Biermann, P. L., & Cassinelli, J. P. 1993, Cosmic Rays, II. Evidence for a magnetic rotator Wolf Rayet star origin. <https://arxiv.org/abs/astro-ph/9305003>
- Boggs, P. T., & Donaldson, J. R. 1989, in Orthogonal distance regression
- Bosnjak, Z., Celotti, A., Ghirlanda, G., Della Valle, M., & Pian, E. 2006, Astronomy & Astrophysics, 447, 121, doi: [10.1051/0004-6361:20052803](https://doi.org/10.1051/0004-6361:20052803)
- Bromberg, O., Nakar, E., Piran, T., & Sari, R. 2013, The Astrophysical Journal, 764, 179, doi: [10.1088/0004-637x/764/2/179](https://doi.org/10.1088/0004-637x/764/2/179)
- Butler, N., Sakamoto, T., Suzuki, M., et al. 2005, The Astrophysical Journal, 621, 884–893, doi: [10.1086/427746](https://doi.org/10.1086/427746)
- Campana, S., Guidorzi, C., Tagliaferri, G., et al. 2007, Astron. Astrophys., 472, 395, doi: [10.1051/0004-6361:20066984](https://doi.org/10.1051/0004-6361:20066984)
- Campana, S., Mangano, V., Blustin, A. J., et al. 2006, Nature, 442, 1008–1010, doi: [10.1038/nature04892](https://doi.org/10.1038/nature04892)
- Campana, S., et al. 2008, Astrophys. J. Lett., 683, L9, doi: [10.1086/591421](https://doi.org/10.1086/591421)
- Cannizzo, J. K., & Gehrels, N. 2009, The Astrophysical Journal, 700, 1047–1058, doi: [10.1088/0004-637x/700/2/1047](https://doi.org/10.1088/0004-637x/700/2/1047)
- Cannizzo, J. K., Troja, E., & Gehrels, N. 2011, The Astrophysical Journal, 734, 35, doi: [10.1088/0004-637x/734/1/35](https://doi.org/10.1088/0004-637x/734/1/35)
- Cano, Z. 2011, PhD thesis. <https://arxiv.org/ftp/arxiv/papers/1208/1208.0307.pdf>
- . 2013, Monthly Notices of the Royal Astronomical Society, 434, 1098, doi: [10.1093/mnras/stt1048](https://doi.org/10.1093/mnras/stt1048)

- Cano, Z. 2014, *ApJ*, 794, 121,
doi: [10.1088/0004-637X/794/2/121](https://doi.org/10.1088/0004-637X/794/2/121)
- Cano, Z., Wang, S.-Q., Dai, Z.-G., & Wu, X.-F. 2017a,
Advances in Astronomy, 2017, 1,
doi: [10.1155/2017/8929054](https://doi.org/10.1155/2017/8929054)
- Cano, Z., de Ugarte Postigo, A., Pozanenko, A., et al. 2014,
Astronomy & Astrophysics, 568, A19,
doi: [10.1051/0004-6361/201423920](https://doi.org/10.1051/0004-6361/201423920)
- Cano, Z., Izzo, L., de Ugarte Postigo, A., et al. 2017b,
Astronomy & Astrophysics, 605, A107,
doi: [10.1051/0004-6361/201731005](https://doi.org/10.1051/0004-6361/201731005)
- Cao, S., Dainotti, M., & Ratra, B. 2022a.
<https://arxiv.org/abs/2201.05245>
- Cao, S., Khadka, N., & Ratra, B. 2022b, *Monthly Notices of the Royal Astronomical Society*, 510, 2928,
doi: [10.1093/mnras/stab3559](https://doi.org/10.1093/mnras/stab3559)
- Chen, K.-J., Moriya, T. J., Woosley, S., et al. 2017, *The Astrophysical Journal*, 839, 85,
doi: [10.3847/1538-4357/aa68a4](https://doi.org/10.3847/1538-4357/aa68a4)
- Corsi, A., Cenko, S. B., Kasliwal, M. M., et al. 2017, *The Astrophysical Journal*, 847, 54,
doi: [10.3847/1538-4357/aa85e5](https://doi.org/10.3847/1538-4357/aa85e5)
- Dado, S., Dar, A., & De Rújula, A. 2002, *Astronomy & Astrophysics*, 393, L25, doi: [10.1051/0004-6361:20021167](https://doi.org/10.1051/0004-6361:20021167)
- Dainotti, M., & Del Vecchio, R. 2017, *New Astronomy Reviews*, 77, 23, doi: [10.1016/j.newar.2017.04.001](https://doi.org/10.1016/j.newar.2017.04.001)
- Dainotti, M., Levine, D., Fraija, N., & Chandra, P. 2021a,
Galaxies, 9, doi: [10.3390/galaxies9040095](https://doi.org/10.3390/galaxies9040095)
- Dainotti, M., Ostrowski, M., & Willingale, R. 2011,
MNRAS, 418, 2202,
doi: [10.1111/j.1365-2966.2011.19433.x](https://doi.org/10.1111/j.1365-2966.2011.19433.x)
- Dainotti, M., Petrosian, V., Willingale, R., et al. 2015,
Monthly Notices of the Royal Astronomical Society, 451,
3898, doi: [10.1093/mnras/stv1229](https://doi.org/10.1093/mnras/stv1229)
- Dainotti, M. G., & Amati, L. 2018, *Publications of the Astronomical Society of the Pacific*, 130, 051001,
doi: [10.1088/1538-3873/aaa8d7](https://doi.org/10.1088/1538-3873/aaa8d7)
- Dainotti, M. G., Bernardini, M. G., Bianco, C. L., et al. 2007, *A&A*, 471, L29, doi: [10.1051/0004-6361:20078068](https://doi.org/10.1051/0004-6361:20078068)
- Dainotti, M. G., Cardone, V. F., & Capozziello, S. 2008,
Monthly Notices of the Royal Astronomical Society: Letters, 391, L79, doi: [10.1111/j.1745-3933.2008.00560.x](https://doi.org/10.1111/j.1745-3933.2008.00560.x)
- Dainotti, M. G., De Simone, B., Schiavone, T., et al. 2021b,
The Astrophysical Journal, 912, 150,
doi: [10.3847/1538-4357/abeb73](https://doi.org/10.3847/1538-4357/abeb73)
- Dainotti, M. G., De Simone, B. D., Schiavone, T., et al. 2022a,
Galaxies, 10, 24, doi: [10.3390/galaxies10010024](https://doi.org/10.3390/galaxies10010024)
- Dainotti, M. G., Hernandez, X., Postnikov, S., et al. 2017a,
848, 88, doi: [10.3847/1538-4357/aa8a6b](https://doi.org/10.3847/1538-4357/aa8a6b)
- Dainotti, M. G., Lenart, A. L., Sarracino, G., et al. 2020a,
The Astrophysical Journal, 904, 97,
doi: [10.3847/1538-4357/abbe8a](https://doi.org/10.3847/1538-4357/abbe8a)
- Dainotti, M. G., Nagataki, S., Maeda, K., Postnikov, S., & Pian, E. 2017b, *Astronomy & Astrophysics*, 600, A98,
doi: [10.1051/0004-6361/201628384](https://doi.org/10.1051/0004-6361/201628384)
- Dainotti, M. G., Nielson, V., Sarracino, G., et al. 2022b,
Optical and X-ray GRB Fundamental Planes as Cosmological Distance Indicators, arXiv,
doi: [10.48550/ARXIV.2203.15538](https://doi.org/10.48550/ARXIV.2203.15538)
- Dainotti, M. G., Petrosian, V., Singal, J., & Ostrowski, M. 2013, *The Astrophysical Journal*, 774, 157,
doi: [10.1088/0004-637x/774/2/157](https://doi.org/10.1088/0004-637x/774/2/157)
- Dainotti, M. G., Postnikov, S., Hernandez, X., & Ostrowski, M. 2016, 825, L20, doi: [10.3847/2041-8205/825/2/l20](https://doi.org/10.3847/2041-8205/825/2/l20)
- Dainotti, M. G., Livermore, S., Kann, D. A., et al. 2020b,
The Astrophysical Journal Letters, 905, L26,
doi: [10.3847/2041-8213/abcd9](https://doi.org/10.3847/2041-8213/abcd9)
- Dall’Osso, S., Stratta, G., Guetta, D., et al. 2011, *A&A*, 526, A121, doi: [10.1051/0004-6361/201014168](https://doi.org/10.1051/0004-6361/201014168)
- Della Valle, M., Malesani, D., Bloom, J. S., et al. 2006, *The Astrophysical Journal*, 642, L103, doi: [10.1086/504636](https://doi.org/10.1086/504636)
- Demianski, M., Piedipalumbo, E., Sawant, D., & Amati, L. 2017, *Astronomy & Astrophysics*, 598, A112,
doi: [10.1051/0004-6361/201628909](https://doi.org/10.1051/0004-6361/201628909)
- Dereli, H., Boér, M., Gendre, B., et al. 2017, *The Astrophysical Journal*, 850, 117,
doi: [10.3847/1538-4357/aa947d](https://doi.org/10.3847/1538-4357/aa947d)
- Duncan, R. C. 2001, *AIP Conference Proceedings*,
doi: [10.1063/1.1419599](https://doi.org/10.1063/1.1419599)
- D’Elia, V., Campana, S., D’Ai, A., et al. 2018, *Astronomy & Astrophysics*, 619, A66,
doi: [10.1051/0004-6361/201833847](https://doi.org/10.1051/0004-6361/201833847)
- Efron, B., & Petrosian, V. 1992, *Astrophysical Journal*, 399, doi: [10.1086/171931](https://doi.org/10.1086/171931)
- Eisenberg, M., Gottlieb, O., & Nakar, E. 2022,
Observational signatures of stellar explosions driven by relativistic jets. <https://arxiv.org/abs/2201.08432>
- Evans, P. A., Beardmore, A. P., Page, K. L., et al. 2009,
MNRAS, 397, 1177,
doi: [10.1111/j.1365-2966.2009.14913.x](https://doi.org/10.1111/j.1365-2966.2009.14913.x)
- Ferrero, P., Kann, D. A., Zeh, A., et al. 2006, *Astronomy & Astrophysics*, 457, 857, doi: [10.1051/0004-6361:20065530](https://doi.org/10.1051/0004-6361:20065530)
- Frail, D. A., Kulkarni, S. R., Sari, R., et al. 2001, *The Astrophysical Journal*, 562, L55, doi: [10.1086/338119](https://doi.org/10.1086/338119)
- Fynbo, J. P. U., Sollerman, J., Hjorth, J., et al. 2004, *The Astrophysical Journal*, 609, 962–971, doi: [10.1086/421260](https://doi.org/10.1086/421260)
- Fynbo, J. P. U., Watson, D., Thöne, C. C., et al. 2006,
Nature, 444, 1047–1049, doi: [10.1038/nature05375](https://doi.org/10.1038/nature05375)

- Galama, T. J., Vreeswijk, P. M., van Paradijs, J., et al. 1998, *Nature*, 395, 670, doi: [10.1038/27150](https://doi.org/10.1038/27150)
- Garnavich, P. M., Stanek, K. Z., Wyrzykowski, L., et al. 2003, *The Astrophysical Journal*, 582, 924, doi: [10.1086/344785](https://doi.org/10.1086/344785)
- Gehrels, N. 2004, *AIP Conference Proceedings*, doi: [10.1063/1.1810924](https://doi.org/10.1063/1.1810924)
- Gendre, B., Galli, A., & Piro, L. 2007, *Astronomy & Astrophysics*, 465, L13–L16, doi: [10.1051/0004-6361:20066896](https://doi.org/10.1051/0004-6361:20066896)
- Gendre, B., Joyce, Q. T., Orange, N. B., et al. 2019, *Monthly Notices of the Royal Astronomical Society*, 486, 2471, doi: [10.1093/mnras/stz1036](https://doi.org/10.1093/mnras/stz1036)
- Germany, L. M., Reiss, D. J., Sadler, E. M., Schmidt, B. P., & Stubbs, C. W. 2000, *The Astrophysical Journal*, 533, 320, doi: [10.1086/308639](https://doi.org/10.1086/308639)
- Ghirlanda, G., Ghisellini, G., & Lazzati, D. 2004, *The Astrophysical Journal*, 616, 331–338, doi: [10.1086/424913](https://doi.org/10.1086/424913)
- Ghirlanda, G., Nava, L., & Ghisellini, G. 2010, *A&A*, 511, A43, doi: [10.1051/0004-6361/200913134](https://doi.org/10.1051/0004-6361/200913134)
- Ghisellini, G., Ghirlanda, G., Mereghetti, S., et al. 2006, *Monthly Notices of the Royal Astronomical Society*, 372, 1699, doi: [10.1111/j.1365-2966.2006.10972.x](https://doi.org/10.1111/j.1365-2966.2006.10972.x)
- Gompertz, B. P., Levan, A. J., & Tanvir, N. R. 2020, *The Astrophysical Journal*, 895, 58, doi: [10.3847/1538-4357/ab8d24](https://doi.org/10.3847/1538-4357/ab8d24)
- Granot, J., Piran, T., & Sari, R. 1999, *The Astrophysical Journal*, 513, 679–689, doi: [10.1086/306884](https://doi.org/10.1086/306884)
- Granot, J., & Sari, R. 2002, *The Astrophysical Journal*, 568, 820–829, doi: [10.1086/338966](https://doi.org/10.1086/338966)
- Granot, J., & van der Horst, A. J. 2014, *Publications of the Astronomical Society of Australia*, 31, e008, doi: [10.1017/pasa.2013.44](https://doi.org/10.1017/pasa.2013.44)
- Guessoum, N., Alarayani, O., Al-Qassimi, K., et al. 2017, *Journal of Physics: Conference Series*, 869, 012080, doi: [10.1088/1742-6596/869/1/012080](https://doi.org/10.1088/1742-6596/869/1/012080)
- Guetta, D., & Valle, M. D. 2007, *The Astrophysical Journal*, 657, L73, doi: [10.1086/511417](https://doi.org/10.1086/511417)
- Guillochon, J., Parrent, J., Kelley, L. Z., & Margutti, R. 2017, *ApJ*, 835, 64, doi: [10.3847/1538-4357/835/1/64](https://doi.org/10.3847/1538-4357/835/1/64)
- Götz, D., Laurent, P., Antier, S., et al. 2014, *Monthly Notices of the Royal Astronomical Society*, 444, 2776–2782, doi: [10.1093/mnras/stu1634](https://doi.org/10.1093/mnras/stu1634)
- Heise, J. 2003, *AIP Conference Proceedings*, doi: [10.1063/1.1579346](https://doi.org/10.1063/1.1579346)
- Hjorth, J. 2013, *Philosophical Transactions of the Royal Society A: Mathematical, Physical and Engineering Sciences*, 371, 20120275, doi: [10.1098/rsta.2012.0275](https://doi.org/10.1098/rsta.2012.0275)
- Hjorth, J., & Bloom, J. S. 2012, *The GRB–supernova connection*, Cambridge University Press.
- <https://www.cambridge.org/core/books/gammaray-bursts/grbsupernova-connection/55BADFF3931C3239FE76146FDB15E145>
- Hu, Y.-D., Castro-Tirado, A. J., Kumar, A., et al. 2021, *Astronomy & Astrophysics*, 646, A50, doi: [10.1051/0004-6361/202039349](https://doi.org/10.1051/0004-6361/202039349)
- Hudec, R., Hudcová, V., & Hroch, F. 1999, *Astronomy and Astrophysics Supplement Series*, 138, 475, doi: [10.1051/aas:1999316](https://doi.org/10.1051/aas:1999316)
- Ito, H., Matsumoto, J., Nagataki, S., et al. 2019, *Nature Communications*, 10, doi: [10.1038/s41467-019-09281-z](https://doi.org/10.1038/s41467-019-09281-z)
- Izzo, L., De Ugarte Postigo, A., Maeda, K., et al. 2019, *Jet cocoon signatures in the early spectra of a gamma-ray burst/supernova*. <https://arxiv.org/pdf/1901.05500.pdf>
- Kaneko, Y., Bostancı, Z. F., Göğüş, E., & Lin, L. 2015, *Monthly Notices of the Royal Astronomical Society*, 452, 824, doi: [10.1093/mnras/stv1286](https://doi.org/10.1093/mnras/stv1286)
- Kann, D. A., Schady, P., Olivares, E. F., et al. 2019, *Astronomy & Astrophysics*, 624, A143, doi: [10.1051/0004-6361/201629162](https://doi.org/10.1051/0004-6361/201629162)
- Kendall, M. 1948, *Rank Correlation Methods* (C. Griffin). <https://books.google.it/books?id=hiBMAAAAMAAJ>
- Khatami, D. K., & Kasen, D. N. 2019, *The Astrophysical Journal*, 878, 56, doi: [10.3847/1538-4357/ab1f09](https://doi.org/10.3847/1538-4357/ab1f09)
- Klose, S., Schmidl, S., Kann, D. A., et al. 2019, *Astronomy & Astrophysics*, 622, A138, doi: [10.1051/0004-6361/201832728](https://doi.org/10.1051/0004-6361/201832728)
- Klotz, A., Gendre, B., Stratta, G., et al. 2008, *Astronomy & Astrophysics*, 483, 847–855, doi: [10.1051/0004-6361:20078677](https://doi.org/10.1051/0004-6361:20078677)
- Kocevski, D., & Liang, E. 2006, *The Astrophysical Journal*, 642, 371, doi: [10.1086/500816](https://doi.org/10.1086/500816)
- Kong, S., Huang, Y., Cheng, K., & Lu, T. 2009, *Science in China Series G: Physics, Mechanics and Astronomy*, 52, 2047–2053, doi: [10.1007/s11433-009-0275-y](https://doi.org/10.1007/s11433-009-0275-y)
- Kouveliotou, C., Meegan, C. A., Fishman, G. J., et al. 1993, *The Astrophysical Journal Letters*, 413, L101–L104, doi: [10.1086/186969](https://doi.org/10.1086/186969)
- Kumar, P., Narayan, R., & Johnson, J. L. 2008a, *Science*, 321, 376–379, doi: [10.1126/science.1159003](https://doi.org/10.1126/science.1159003)
- . 2008b, *MNRAS*, 388, 1729, doi: [10.1111/j.1365-2966.2008.13493.x](https://doi.org/10.1111/j.1365-2966.2008.13493.x)
- Kumar, P., & Zhang, B. 2015, *Physics Reports*, 561, 1–109, doi: [10.1016/j.physrep.2014.09.008](https://doi.org/10.1016/j.physrep.2014.09.008)
- Levan, A. J., Tanvir, N. R., Fruchter, A. S., et al. 2014, *The Astrophysical Journal*, 792, 115, doi: [10.1088/0004-637x/792/2/115](https://doi.org/10.1088/0004-637x/792/2/115)

- Li, L.-X. 2006a, Monthly Notices of the Royal Astronomical Society, 372, 1357, doi: [10.1111/j.1365-2966.2006.10943.x](https://doi.org/10.1111/j.1365-2966.2006.10943.x)
- . 2006b, Monthly Notices of the Royal Astronomical Society, 372, 1357, doi: [10.1111/j.1365-2966.2006.10943.x](https://doi.org/10.1111/j.1365-2966.2006.10943.x)
- Li, L.-X. 2008a, MNRAS, 388, 603, doi: [10.1111/j.1365-2966.2008.13461.x](https://doi.org/10.1111/j.1365-2966.2008.13461.x)
- . 2008b, The GRB-Supernova Connection, doi: [10.1063/1.3027928](https://doi.org/10.1063/1.3027928)
- Li, W., Filippenko, A., Van Dyk, S., et al. 2002, A Hubble Space Telescope snapshot survey of nearby supernovae. <https://arxiv.org/pdf/astro-ph/0201228.pdf>
- Liang, E., Racusin, J. L., Zhang, B., Zhang, B., & Burrows, D. N. 2008, The Astrophysical Journal, 675, 528–552, doi: [10.1086/524701](https://doi.org/10.1086/524701)
- Liang, E., & Zhang, B. 2005, 633, 611, doi: [10.1086/491594](https://doi.org/10.1086/491594)
- Liang, E., Zhang, B., Virgili, F., & Dai, Z. G. 2007, The Astrophysical Journal, 662, 1111, doi: [10.1086/517959](https://doi.org/10.1086/517959)
- Lin, J., Lu, R.-J., Lin, D.-B., & Wang, X.-G. 2020, The Astrophysical Journal, 895, 46, doi: [10.3847/1538-4357/ab88a7](https://doi.org/10.3847/1538-4357/ab88a7)
- Lloyd, N. M., & Petrosian, V. 2000, The Astrophysical Journal, 543, 722, doi: [10.1086/317125](https://doi.org/10.1086/317125)
- Lloyd-Ronning, N., Hurtado, V. U., Aykutalp, A., Johnson, J., & Ceccobello, C. 2020, Monthly Notices of the Royal Astronomical Society, 494, 4371, doi: [10.1093/mnras/staa1057](https://doi.org/10.1093/mnras/staa1057)
- Lloyd-Ronning, N. M., Aykutalp, A., & Johnson, J. L. 2019, Monthly Notices of the Royal Astronomical Society, 488, 5823, doi: [10.1093/mnras/stz2155](https://doi.org/10.1093/mnras/stz2155)
- Lyman, J. D., Bersier, D., James, P. A., et al. 2016, Monthly Notices of the Royal Astronomical Society, 457, 328, doi: [10.1093/mnras/stv2983](https://doi.org/10.1093/mnras/stv2983)
- Lü, H.-J., Lan, L., Zhang, B., et al. 2018, The Astrophysical Journal, 862, 130, doi: [10.3847/1538-4357/aacd03](https://doi.org/10.3847/1538-4357/aacd03)
- Madjaz, M., Li, W. D., Garnavich, P., et al. 1999, IAUC 7268: 1999eb; 1999ec; 1999dj. <http://www.cbat.eps.harvard.edu/iauc/07200/07268.html#Item2>
- Malmquist, K. G. 1922, Meddelanden från Lunds Astronomiska Observatorium Serie I, 100, 1
- Martone, R., Izzo, L., Della Valle, M., et al. 2017, Astronomy & Astrophysics, 608, A52, doi: [10.1051/0004-6361/201730704](https://doi.org/10.1051/0004-6361/201730704)
- Mazets, E. P., Golenetskii, S. V., Ilinskii, V. N., et al. 1981, Ap&SS, 80, 3, doi: [10.1007/BF00649140](https://doi.org/10.1007/BF00649140)
- Mazzali, P. A. 2011, Proceedings of the International Astronomical Union, 7, 75, doi: [10.1017/s1743921312012720](https://doi.org/10.1017/s1743921312012720)
- Mazzali, P. A., Valenti, S., Della Valle, M., et al. 2008, Science, 321, 1185, doi: [10.1126/science.1158088](https://doi.org/10.1126/science.1158088)
- Melandri, A., Pian, E., D'Elia, V., et al. 2014, A&A, 567, A29, doi: [10.1051/0004-6361/201423572](https://doi.org/10.1051/0004-6361/201423572)
- Melandri, A., Malesani, D. B., Izzo, L., et al. 2019, Monthly Notices of the Royal Astronomical Society, 490, 5366, doi: [10.1093/mnras/stz2900](https://doi.org/10.1093/mnras/stz2900)
- Messzaros, P. 2000, AIP Conference Proceedings, doi: [10.1063/1.1361591](https://doi.org/10.1063/1.1361591)
- Mészáros, P. 2001, Progress of Theoretical Physics Supplement, 143, 33, doi: [10.1143/PTPS.143.33](https://doi.org/10.1143/PTPS.143.33)
- Minaev, P. Y., & Pozanenko, A. S. 2019, Monthly Notices of the Royal Astronomical Society, 492, 1919, doi: [10.1093/mnras/stz3611](https://doi.org/10.1093/mnras/stz3611)
- Modjaz, M., Li, W., Butler, N., et al. 2009, The Astrophysical Journal, 702, 226, doi: [10.1088/0004-637x/702/1/226](https://doi.org/10.1088/0004-637x/702/1/226)
- Moriya, T. J., Marchant, P., & Blinnikov, S. I. 2020, Astronomy & Astrophysics, 641, L10, doi: [10.1051/0004-6361/202038903](https://doi.org/10.1051/0004-6361/202038903)
- Nagataki, S. 2009, The Astrophysical Journal, 704, 937–950, doi: [10.1088/0004-637x/704/2/937](https://doi.org/10.1088/0004-637x/704/2/937)
- Nakauchi, D., Kashiyama, K., Suwa, Y., & Nakamura, T. 2013, The Astrophysical Journal, 778, 67, doi: [10.1088/0004-637x/778/1/67](https://doi.org/10.1088/0004-637x/778/1/67)
- Nicholl, M. 2021, Astronomy & Geophysics, 62, 5.34, doi: [10.1093/astrogeo/atab092](https://doi.org/10.1093/astrogeo/atab092)
- Nicolas, N., Rigault, M., Copin, Y., et al. 2021, Astronomy & Astrophysics, 649, A74, doi: [10.1051/0004-6361/202038447](https://doi.org/10.1051/0004-6361/202038447)
- Nomoto, K., Moriya, T., Tominaga, N., & Suzuki, T. 2010, AIP Conference Proceedings, 1279, 60, doi: [10.1063/1.3509354](https://doi.org/10.1063/1.3509354)
- Nomoto, K., Tominaga, N., Tanaka, M., Maeda, K., & Umeda, H. 2008, in Massive Stars as Cosmic Engines, ed. F. Bresolin, P. A. Crowther, & J. Puls, Vol. 250, 463–470, doi: [10.1017/S1743921308020838](https://doi.org/10.1017/S1743921308020838)
- Nomoto, K., Mazzali, P. A., Nakamura, T., et al. 2000, AIP Conf. Proc., 526, 622, doi: [10.1063/1.1361611](https://doi.org/10.1063/1.1361611)
- Oates, S. R., Page, M. J., De Pasquale, M., et al. 2012, MNRAS, 426, L86, doi: [10.1111/j.1745-3933.2012.01331.x](https://doi.org/10.1111/j.1745-3933.2012.01331.x)
- Ofek, E. O., Cenko, S. B., Gal-Yam, A., et al. 2007, The Astrophysical Journal, 662, 1129, doi: [10.1086/518082](https://doi.org/10.1086/518082)
- Pearson, K. 1901, The London, Edinburgh, and Dublin Philosophical Magazine and Journal of Science, 2, 559, doi: [10.1080/14786440109462720](https://doi.org/10.1080/14786440109462720)
- Perley, D. A., Bloom, J. S., Klein, C. R., et al. 2010, Monthly Notices of the Royal Astronomical Society, 406, 2473, doi: [10.1111/j.1365-2966.2010.16772.x](https://doi.org/10.1111/j.1365-2966.2010.16772.x)
- Perna, R., Lazzati, D., & Cantiello, M. 2018, The Astrophysical Journal, 859, 48, doi: [10.3847/1538-4357/aabcc1](https://doi.org/10.3847/1538-4357/aabcc1)

- Petrosian, V., Bouvier, A., & Ryde, F. 2009, Gamma-ray Bursts as Cosmological Tools.
<https://arxiv.org/pdf/0909.5051.pdf>
- Phillips, M. M. 1993, *The Astrophysical Journal Letters*, 413, L105, doi: [10.1086/186970](https://doi.org/10.1086/186970)
- Pian, E. 2005, in *Astronomical Society of the Pacific Conference Series*, Vol. 342, 1604-2004: Supernovae as Cosmological Lighthouses, ed. M. Turatto, S. Benetti, L. Zampieri, & W. Shea, 315
- Pian, E., Giommi, P., Amati, L., et al. 2004, *Advances in Space Research*, 34, 2711–2714, doi: [10.1016/j.asr.2003.04.072](https://doi.org/10.1016/j.asr.2003.04.072)
- Pian, E., Mazzali, P. A., Masetti, N., et al. 2006, *Nature*, 442, 1011–1013, doi: [10.1038/nature05082](https://doi.org/10.1038/nature05082)
- Pian, E., D’Avanzo, P., Benetti, S., et al. 2017, *Nature*, 551, 67–70, doi: [10.1038/nature24298](https://doi.org/10.1038/nature24298)
- Piran, T. 1999, *Physics Reports*, 314, 575–667, doi: [10.1016/s0370-1573\(98\)00127-6](https://doi.org/10.1016/s0370-1573(98)00127-6)
- Piran, T. 2000, *PhR*, 333, 529, doi: [10.1016/S0370-1573\(00\)00036-3](https://doi.org/10.1016/S0370-1573(00)00036-3)
- Piro, L., Troja, E., Gendre, B., et al. 2014, *ApJL*, 790, L15, doi: [10.1088/2041-8205/790/2/L15](https://doi.org/10.1088/2041-8205/790/2/L15)
- Prentice, S. J., Mazzali, P. A., Pian, E., et al. 2016, *Monthly Notices of the Royal Astronomical Society*, 458, 2973, doi: [10.1093/mnras/stw299](https://doi.org/10.1093/mnras/stw299)
- Price, P. A., Kulkarni, S. R., Schmidt, B. P., et al. 2003, *The Astrophysical Journal*, 584, 931, doi: [10.1086/345734](https://doi.org/10.1086/345734)
- Qin, Y.-P., & Chen, Z.-F. 2013, *Monthly Notices of the Royal Astronomical Society*, 430, 163, doi: [10.1093/mnras/sts547](https://doi.org/10.1093/mnras/sts547)
- Rastinejad, J. C., Gompertz, B. P., Levan, A. J., et al. 2022, *A Kilonova Following a Long-Duration Gamma-Ray Burst at 350 Mpc*, arXiv, doi: [10.48550/ARXIV.2204.10864](https://doi.org/10.48550/ARXIV.2204.10864)
- Rea, N., Gullón, M., Pons, J. A., et al. 2015, *ApJ*, 813, 92, doi: [10.1088/0004-637X/813/2/92](https://doi.org/10.1088/0004-637X/813/2/92)
- Rhodes, L., Fender, R., Williams, D. R. A., & Mooley, K. 2021, *Monthly Notices of the Royal Astronomical Society*, 503, 2966, doi: [10.1093/mnras/stab640](https://doi.org/10.1093/mnras/stab640)
- Rigon, L., Turatto, M., Benetti, S., et al. 2003, *Monthly Notices of the Royal Astronomical Society*, 340, 191, doi: [10.1046/j.1365-8711.2003.06282.x](https://doi.org/10.1046/j.1365-8711.2003.06282.x)
- Rossi, A., Rothberg, B., Palazzi, E., et al. 2021, submitted to *ApJ*, 1, doi: [arXiv:2105.03829](https://arxiv.org/abs/2105.03829)
- Rowlinson, A., Gompertz, B. P., Dainotti, M., et al. 2014, *Monthly Notices of the Royal Astronomical Society*, 443, 1779, doi: [10.1093/mnras/stu1277](https://doi.org/10.1093/mnras/stu1277)
- Rowlinson, A., O’Brien, P. T., Metzger, B. D., Tanvir, N. R., & Levan, A. J. 2013, *MNRAS*, 430, 1061, doi: [10.1093/mnras/sts683](https://doi.org/10.1093/mnras/sts683)
- Rueda, J. A., & Ruffini, R. 2012, *The Astrophysical Journal*, 758, L7, doi: [10.1088/2041-8205/758/1/17](https://doi.org/10.1088/2041-8205/758/1/17)
- Ruffini, R., Bianco, C. L., Fraschetti, F., Xue, S.-S., & Chardonnet, P. 2001, *The Astrophysical Journal*, 555, L117, doi: [10.1086/323177](https://doi.org/10.1086/323177)
- Ruffini, R., Rueda, J. A., Muccino, M., et al. 2016, *The Astrophysical Journal*, 832, 136, doi: [10.3847/0004-637x/832/2/136](https://doi.org/10.3847/0004-637x/832/2/136)
- Ruffini, R., Moradi, R., Aimuratov, Y., et al. 2021, GRB 210210A as a BdHN II, NASA.
<https://gcn.gsfc.nasa.gov/gcn/gcn3/29481.gcn3>
- Sakamoto, T. 2004, *AIP Conference Proceedings*, doi: [10.1063/1.1810811](https://doi.org/10.1063/1.1810811)
- Sakamoto, T., Barthelmy, S. D., Barbier, L., et al. 2008, *The Astrophysical Journal Supplement Series*, 175, 179–190, doi: [10.1086/523646](https://doi.org/10.1086/523646)
- Schady, P. 2017, Gamma-ray bursts and their use as cosmic probes. <https://arxiv.org/abs/1707.05214>
- Schaerer, D., de Koter, A., & Schmutz, W. 1994, Combined Stellar Structure and Atmosphere Models: Exploratory Results for Wolf-Rayet Stars.
<https://arxiv.org/abs/astro-ph/9410046>
- Schmidt, M. 2005, *Il Nuovo Cimento*, 28 (2005), 347, doi: [10.1393/ncc/i2005-10057-9](https://doi.org/10.1393/ncc/i2005-10057-9)
- Schulze, S., Malesani, D., Cucchiara, A., et al. 2014, *A&A*, 566, A102, doi: [10.1051/0004-6361/201423387](https://doi.org/10.1051/0004-6361/201423387)
- Shahmoradi, A., & Nemiroff, R. J. 2015, *Monthly Notices of the Royal Astronomical Society*, 451, 126, doi: [10.1093/mnras/stv714](https://doi.org/10.1093/mnras/stv714)
- Singal, J., Petrosian, V., Lawrence, A., & Stawarz, L. 2011, *The Astrophysical Journal*, 743, 104, doi: [10.1088/0004-637x/743/2/104](https://doi.org/10.1088/0004-637x/743/2/104)
- Soderberg, A. M., Nakar, E., Berger, E., & Kulkarni, S. R. 2006a, *The Astrophysical Journal*, 638, 930–937, doi: [10.1086/499121](https://doi.org/10.1086/499121)
- Soderberg, A. M., Kulkarni, S. R., Nakar, E., et al. 2006b, *Nature*, 442, 1014–1017, doi: [10.1038/nature05087](https://doi.org/10.1038/nature05087)
- Soderberg, A. M., Berger, E., Page, K. L., et al. 2008, *Nature*, 453, 469, doi: [10.1038/nature06997](https://doi.org/10.1038/nature06997)
- Sollerman, J., Jaunsen, A. O., Fynbo, J. P. U., et al. 2006, *A&A*, 454, 503, doi: [10.1051/0004-6361:20065226](https://doi.org/10.1051/0004-6361:20065226)
- Spearman, C. 1904, *The American Journal of Psychology*, 15, 72. <http://www.jstor.org/stable/1412159>
- Starling, R. L. C., Wiersema, K., Levan, A. J., et al. 2010, *Monthly Notices of the Royal Astronomical Society*, 411, 2792, doi: [10.1111/j.1365-2966.2010.17879.x](https://doi.org/10.1111/j.1365-2966.2010.17879.x)
- Stratta, G., Dainotti, M. G., Dall’Osso, S., Hernandez, X., & De Cesare, G. 2018, *Astrophys. J.*, 869, 155, doi: [10.3847/1538-4357/aadd8f](https://doi.org/10.3847/1538-4357/aadd8f)

- Stritzinger, M., Hamuy, M., Suntzeff, N. B., et al. 2002, *The Astronomical Journal*, 124, 2100–2117, doi: [10.1086/342544](https://doi.org/10.1086/342544)
- Sultana, J., Kazanas, D., & Mastichiadis, A. 2013, *The Astrophysical Journal*, 779, 16, doi: [10.1088/0004-637x/779/1/16](https://doi.org/10.1088/0004-637x/779/1/16)
- Suzuki, A., Maeda, K., & Shigeyama, T. 2019, *The Astrophysical Journal*, 870, 38, doi: [10.3847/1538-4357/aaef85](https://doi.org/10.3847/1538-4357/aaef85)
- Tanaka, M., Moriya, T. J., Yoshida, N., & Nomoto, K. 2012, *Monthly Notices of the Royal Astronomical Society*, 422, 2675–2684, doi: [10.1111/j.1365-2966.2012.20833.x](https://doi.org/10.1111/j.1365-2966.2012.20833.x)
- Terlevich, R., & al. e. 199, IAUC 7269: 1999eb, GRB 991002; 1999ec; 1999do, www.cbat.eps.harvard.edu. <http://www.cbat.eps.harvard.edu/iauc/07200/07269.html#Item1>
- Toffano, M., Ghirlanda, G., Nava, L., et al. 2021, *Astronomy & Astrophysics*, 652, A123, doi: [10.1051/0004-6361/202141032](https://doi.org/10.1051/0004-6361/202141032)
- Tominaga, N., Deng, J., Mazzali, P. A., et al. 2004, *The Astrophysical Journal*, 612, L105–L108, doi: [10.1086/424841](https://doi.org/10.1086/424841)
- Tominaga, N., Maeda, K., Umeda, H., et al. 2007, *The Astrophysical Journal*, 657, L77, doi: [10.1086/513193](https://doi.org/10.1086/513193)
- Troja, E., Piro, L., van Eerten, H., et al. 2017, *Nature*, 551, 71–74, doi: [10.1038/nature24290](https://doi.org/10.1038/nature24290)
- Tsutsui, R., & Shigeyama, T. 2013, *Publications of the Astronomical Society of Japan*, 65, doi: [10.1093/pasj/65.3.L3](https://doi.org/10.1093/pasj/65.3.L3)
- Tsutsui, R., Yonetoku, D., Nakamura, T., Takahashi, K., & Moribara, Y. 2013, *Monthly Notices of the Royal Astronomical Society*, 431, 1398–1404, doi: [10.1093/mnras/stt262](https://doi.org/10.1093/mnras/stt262)
- Tsvetkova, A., Frederiks, D., Svinkin, D., et al. 2021, *The Astrophysical Journal*, 908, 83, doi: [10.3847/1538-4357/abd569](https://doi.org/10.3847/1538-4357/abd569)
- Turatto, M., Suzuki, T., Mazzali, P. A., et al. 2000, *The Astrophysical Journal*, 534, L57, doi: [10.1086/312653](https://doi.org/10.1086/312653)
- Umeda, H., Tominaga, N., Maeda, K., & Nomoto, K. 2005, *The Astrophysical Journal*, 633, L17–L20, doi: [10.1086/498136](https://doi.org/10.1086/498136)
- Usov, V. V. 1994, *Hydrodynamics and High-Energy Physics of WR Colliding Winds*. <https://arxiv.org/abs/astro-ph/9405067>
- van Eerten, H. 2014a, *MNRAS*, 442, 3495, doi: [10.1093/mnras/stu1025](https://doi.org/10.1093/mnras/stu1025)
- van Eerten, H. J. 2014b, *MNRAS*, 445, 2414, doi: [10.1093/mnras/stu1921](https://doi.org/10.1093/mnras/stu1921)
- Virgili, F. J., Liang, E.-W., & Zhang, B. 2009, *Monthly Notices of the Royal Astronomical Society*, 392, 91–103, doi: [10.1111/j.1365-2966.2008.14063.x](https://doi.org/10.1111/j.1365-2966.2008.14063.x)
- Virgili, F. J., Mundell, C. G., Pal'shin, V., et al. 2013, *The Astrophysical Journal*, 778, 54, doi: [10.1088/0004-637x/778/1/54](https://doi.org/10.1088/0004-637x/778/1/54)
- von Kienlin, A., Meegan, C. A., Paciesas, W. S., et al. 2020, *The Astrophysical Journal*, 893, 46, doi: [10.3847/1538-4357/ab7a18](https://doi.org/10.3847/1538-4357/ab7a18)
- Wang, L., & Wheeler, J. C. 1998, *ApJL*, 504, L87, doi: [10.1086/311580](https://doi.org/10.1086/311580)
- Wang, Y., Rueda, J. A., Ruffini, R., et al. 2019, *Astrophys. J.*, 874, 39, doi: [10.3847/1538-4357/ab04f8](https://doi.org/10.3847/1538-4357/ab04f8)
- Waxman, E., Meszaros, P., & Campana, S. 2007, *American Astronomical Society*, 667, 351, doi: [10.1086/520715](https://doi.org/10.1086/520715)
- Willingale, R., O'Brien, P. T., Osborne, J. P., et al. 2007, *The Astrophysical Journal*, 662, 1093, doi: [10.1086/517989](https://doi.org/10.1086/517989)
- Woosley, S., & Bloom, J. 2006, *Annual Review of Astronomy and Astrophysics*, 44, 507–556, doi: [10.1146/annurev.astro.43.072103.150558](https://doi.org/10.1146/annurev.astro.43.072103.150558)
- Xu, F., Tang, C.-H., Geng, J.-J., et al. 2021, *The Astrophysical Journal*, 920, 135, doi: [10.3847/1538-4357/ac158a](https://doi.org/10.3847/1538-4357/ac158a)
- Yamazaki, R. 2008, *The Astrophysical Journal*, 690, L118–L121, doi: [10.1088/0004-637x/690/2/l118](https://doi.org/10.1088/0004-637x/690/2/l118)
- Yonetoku, D., Murakami, T., Nakamura, T., et al. 2004, 609, 935, doi: [10.1086/421285](https://doi.org/10.1086/421285)
- Zhang, B.-B., Zhang, B., Sun, H., et al. 2018a, *Nature Communications*, 9, doi: [10.1038/s41467-018-02847-3](https://doi.org/10.1038/s41467-018-02847-3)
- Zhang, B.-B., Liu, Z.-K., Peng, Z.-K., et al. 2021, *Nature Astronomy*, doi: [10.21203/rs.3.rs-131126/v1](https://doi.org/10.21203/rs.3.rs-131126/v1)
- Zhang, B. T., Murase, K., Kimura, S. S., Horiuchi, S., & Mészáros, P. 2018b, *Physical Review D*, 97, doi: [10.1103/physrevd.97.083010](https://doi.org/10.1103/physrevd.97.083010)
- Zhang, W., & Woosley, S. E. 2002, *Relativistic Jets from Collapsars: Gamma-Ray Bursts*. <https://arxiv.org/abs/astro-ph/0209482>
- Zhang, Z.-D., Yu, Y.-W., & Liu, L.-D. 2022, The effects of a magnetar engine on the gamma-ray burst-associated supernovae: Application to double-peaked SN 2006aj, arXiv, doi: [10.48550/ARXIV.2204.11092](https://doi.org/10.48550/ARXIV.2204.11092)
- Zhao, W., Zhang, J.-C., Zhang, Q.-X., et al. 2020, *The Astrophysical Journal*, 900, 112, doi: [10.3847/1538-4357/aba43a](https://doi.org/10.3847/1538-4357/aba43a)

Table 7. Observable characteristics of GRB and SNe

GRB ID	SN ID	GRB Type	SN Type	z	T_{90} (s)	$E_{\gamma, \text{iso}}$ (10^{52} erg)	E_{p}^* (keV)	$L_{\gamma, \text{iso}}$ (10^{50} erg/s)	Grade	$L_{\text{p,bol}}$ (10^{42} erg/s)
910423	1991aa	...	Ib	0.011	208.6 ± 1.1
951107C	1995bc	...	II	0.0477	43.52 ± 5.961
960221	1996N	...	Ib	...	31.328 ± 4.868
960925	1996at	...	Ic-Ib/c	0.09	1.792 ± 0.453
961218	1997B	GRB	Ic-Ib/c	0.01	8.768 ± 0.932
970228	0.695	56	1.6 ^{+0.12} _{-0.12}	195 ⁺⁶⁴ ₋₆₄	4.84	C	...
970508	Ib/c	0.835	23.104 ± 3.789	0.546	145 ⁺⁴³ ₋₄₃	4.34	E	...
970514	1997cy	INT	II	0.0633	1.28 ± 0.771	0.0004	...	0.0332	C	18.6
971013	1997dq	...	Ib	0.0033	12.288 ± 5.514
971115	1997ef	...	Ic	0.01169	C	...
971120	1997ei	...	Ic	0.0106	13.632 ± 2.241	B	...
971221	1997ey	...	Ia	0.58	1.02 ± 0.2	E	...
980326	...	GRB	...	1	9	0.48 ^{+0.09} _{-0.09}	71 ⁺³⁶ ₋₃₆	10.7	D	...
980425	1998bw	IIGRB	Ic	0.00867	18	0.000086 ^{+0.00002} _{-0.00002}	55 ⁺²¹ ₋₂₁	0.000482	A	7.33
980525	1998ce	...	II	...	39.68 ± 2.433
980703	0.967	108.352 ± 2.625	7.41683 ^{+0.714875} _{-0.714875}	503 ⁺⁶⁴ ₋₆₄	28	D	...
980910	1999E	...	II	0.0261	0.72 ± 0.3	B	10
990712	...	GRB	...	0.4331	19	0.67 ^{+0.13} _{-0.13}	93 ⁺¹⁵ ₋₁₅	5.05	C	...
990902	1999dp	...	II	0.016	19.2 ± 5
991002	1999eb	0.018113	1.918 ± 1.995
991021	1999ex	...	Ic	0.011
991208	...	GRB	...	0.7063	60	22.3 ^{+1.8} _{-1.8}	313 ⁺³¹ ₋₃₁	63.4	E	...
000114	2000C	...	Ic	0.012	0.579 ± 0.035
000418	1.1185	2.288 ± 0.92	9.57 ^{+0.49} _{-0.49}	284 ⁺²¹ ₋₂₁	886	D	...
000911	...	GRB	...	1.0585	500	67 ⁺¹⁴ ₋₁₄	1859 ⁺³⁷¹ ₋₃₇₁	27.5	E	...
011121	2001ke	GRB	II	0.362	47	7.8 ^{+2.1} _{-2.1}	1060 ⁺²⁷⁵ ₋₂₇₅	22.6	B	5.9
020405	...	GRB	...	0.68986	40	10 ^{+0.9} _{-0.9}	354 ⁺¹⁰ ₋₁₀	42.2	C	...
020903	...	IIGRB	...	0.2506	3.3	0.0011 ^{+0.0006} _{-0.0006}	3.37 ^{+1.79} _{-1.79}	0.042	B	...
021211	2002lt	GRB	Ic	1.004	2.8	1.12 ^{+0.13} _{-0.13}	108 ⁺²⁶ ₋₆₀	80.2	B	...
030329	2003dh	GRB	Ic-HN	0.16367	22.76 ± 0.5	1.5 ^{+0.3} _{-0.3}	113.3 ^{+2.3} _{-2.3}	7.7	A	10.1
030723	...	XRF	...	0.38	28.3 ± 2.5	0.021 ^{+0.087} _{-0.016}	< 0.023	0.0845	D	...
031203	2003lw	INT	Ic	0.10536	37	0.0086 ^{+0.004} _{-0.004}	158 ⁺⁵¹ ₋₅₁	0.0255	A	12.6
040924	...	GRB	...	0.858	2.39 ± 0.24	0.95 ^{+0.09} _{-0.09}	102 ⁺³⁵ ₋₃₅	73.8	C	...
041006	...	GRB	...	0.716	18	3 ^{+0.9} _{-0.9}	98 ⁺²⁰ ₋₂₀	28.6	C	...
050416A	...	GRB	...	0.6528	2.4 ± 0.2	0.1 ^{+0.01} _{-0.01}	25.1 ^{+4.2} _{-4.2}	6.89	D	...
050525A	2005nc	GRB	Ic	0.606	8.84 ± 0.5	2.5 ^{+0.43} _{-0.43}	127 ⁺¹⁰ ₋₁₀	45.4	B	...

Table 7 continued on next page

Table 7 (*continued*)

GRB ID	SN ID	GRB Type	SN Type	z	T_{90} (s)	$E_{\gamma,\text{iso}}$ (10^{52} erg)	E_{p}^* (keV)	$L_{\gamma,\text{iso}}$ (10^{50} erg/s)	Grade	$L_{\text{p,bol}}$ (10^{42} erg/s)
050824	...	GRB	...	0.8281	25 ± 5	0.1905 ^{+0.1495} _{-0.1495}	21.5 ^{+10.5} _{-10.5}	1.39	E	...
060218	2006aj	IIGRB	Ic-BL	0.03342	2100 ± 100	0.0053 ^{+0.0003} _{-0.0003}	4.9 ^{+0.3} _{-0.3}	0.00026	A	6.47
060729	...	GRB	...	0.5428	115 ± 10	1.6 ^{+0.6} _{-0.6}	77 ⁺³⁸ ₋₃₈	2.14	D	...
060904B	...	GRB	...	0.7029	192 ± 5	2.4 ^{+0.2} _{-0.2}	163 ⁺³¹ ₋₃₁	2.12	C	...
070419A	...	INT	...	0.9705	116 ± 6	0.16	< 69	27.1	D	...
071025	4.88	109 ± 2	65	1023.3 ^{+204.99} _{-204.99}	351	E	...
071112C	0.823	15 ± 2	1.18 ^{+0.19} _{-0.19}	740 ⁺³²⁶ ₋₃₂₆	74.2	C	5.4
080109	2008D	XRF	Ib	0.006494	470 ± 30	0.0000013	0.1685 ^{+0.1315} _{-0.1315}	0.000000278	A	1.66
080319B	...	GRB	...	0.9371	124.86	114 ⁺⁹ ₋₉	1261 ⁺⁶⁵ ₋₆₅	176	C	...
081007A	2008hw	GRB	Ic	0.5295	9.01	0.15 ^{+0.04} _{-0.04}	61 ⁺¹⁵ ₋₁₅	2.54	B	14
090618	...	GRB	...	0.54	113.2 ± 0.6	25.7 ⁺⁵ ₋₅	288 ^{+9.2} _{-9.2}	34.9	C	...
091112T	2009nz	GRB	Ic-BL	0.49044	7.42	1.5 ^{+0.2} _{-0.2}	51 ⁺⁵ ₋₅	30.1	B	12
100316D	2010bh	IIGRB	Ic	0.0592	1300	> 0.0059	26 ⁺¹⁶ ₋₁₆	0.00048	A	5.67
100418A	...	GRB	...	0.6239	8 ± 2	0.099 ^{+0.063} _{-0.063}	47.1 ^{+3.2} _{-3.2}	2	DE	...
101219B	2010ma	GRB	Ic	0.55185	51	0.42 ^{+0.05} _{-0.05}	108 ⁺¹² ₋₁₂	1.27	AB	15
101225A	...	ULGRB	...	0.847	1088 ± 20	1.2 ^{+0.3} _{-0.3}	70 ⁺³⁷ ₋₃₇	0.0316	D	...
111209A	2011kl	ULGRB	SLSN	0.67702	10000	58.2 ^{+7.3} _{-7.3}	520 ⁺⁸⁹ ₋₈₉	0.976	AB	29.1
111211A	0.478	15	0.74	...	7.3	BC	...
111228A	...	GRB	...	0.71627	101.2 ± 5.42	4.2 ^{+0.6} _{-0.6}	58.4 ^{+6.9} _{-6.9}	7.12	E	6.76
120422A	2012bz	GRB	Ic	0.28253	5.4 ± 1.4	0.024 ^{+0.008} _{-0.008}	< 72	57	A	14.8
120714B	2012eb	INT	Ib/c	0.3984	159 ± 34	0.0394 ^{+0.0195} _{-0.0195}	69 ⁺⁴³ ₋₄₃	0.0522	B	6.17
120729A	...	GRB	...	0.8	71.5 ± 17.5	2.3 ^{+1.5} _{-1.5}	559 ⁺⁵⁷ ₋₅₇	5.79	DE	...
130215A	2013ez	GRB	Ic	0.597	65.7 ± 10.8	3.1 ^{+1.6} _{-1.6}	248 ⁺¹⁰¹ ₋₁₀₁	7.53	B	...
130427A	2013cq	GRB	Ic	0.3399	162.83 ± 1.36	81 ⁺¹⁰ ₋₁₀	1415 ⁺¹³ ₋₁₃	6.65E+52	B	9.12
130702A	2013dx	INT	Ic	0.145	58.881	0.0634 ^{+0.013} _{-0.013}	17.2 ^{+5.7} _{-5.7}	0.124	A	10.8
130831A	2013fu	GRB	Ib/c	0.479	32.5 ± 2.5	0.46 ^{+0.02} _{-0.02}	79.9 ^{+10.4} _{-13.3}	2.09	AB	6.92
140206A	2.739	93.2 ± 13.5	240 ⁺² ₋₂	1780 ⁺¹²⁰ ₋₁₂₀	963
140606B	iPTF14bfu	GRB	Ic-BL	0.384	22.78 ± 2.06	0.347 ^{+0.02} _{-0.02}	352 ⁺⁴⁶ ₋₃₇	2.1	AB	...
150818A	...	INT	...	0.285	123.3 ± 31.3	0.1 ^{+0.02} _{-0.02}	128 ⁺¹³ ₋₁₃	0.103	B	...
161219B	2016jea	INT	Ic	0.1475	6.94 ± 0.79	0.0085 ^{+0.0043} _{-0.0043}	71 ^{+19.3} _{-32.2}	0.141	B	4.6
161228B	iPTF17cw	...	Ic-BL	0.093	8.5 ± 0.5	0.023 ^{+0.006} _{-0.006}	214 ⁺²⁶ ₋₂₆	18.3
171010A	2017htp	...	Ic-BL	0.3285	107.266 ± 0.81	18 ^{+0.55} _{-0.55}	227 ⁺⁷ ₋₇	22.3	A	...
171205A	2017iuk	...	Ic-BL	0.0368	189.4 ± 35	0.00218 ^{+0.00063} _{-0.0005}	125 ⁺¹⁴¹ ₋₁₄₁	0.001193	B	...
180720B	0.653	48.897 ± 0.362	33.97 ^{+0.01} _{-0.01}	472 ⁺¹⁵ ₋₁₄	115
180728A	2018fp	XRF	Ic	0.117	8.68 ± 0.3	0.233 ^{+0.1} _{-0.1}	108 ⁺⁸ ₋₇	3	B	...
190114C	2019jrj	0.4245	361.5 ± 11.7	27.03 ^{+0.24} _{-0.24}	929.3 ^{+9.4} _{-9.4}	10.7
190829A	2019oyw	...	Ic-BL	0.0785	58.2 ± 8.9	0.018	140.205 ^{+21.57} _{-21.57}	0.0334	B	...

Table 7 *continued on next page*

Table 7 (*continued*)

GRB ID	SN ID	GRB Type	SN Type	z	T_{90} (s)	$E_{\gamma,\text{iso}}$ (10^{52} erg)	E_p^* (keV)	$L_{\gamma,\text{iso}}$ (10^{50} erg/s)	Grade	$L_{p,\text{bol}}$ (10^{42} erg/s)
200826A	...	GRB	...	0.748577	1.14 ± 0.13	$0.709^{+0.028}_{-0.028}$	$210.33^{+6.87}_{-6.42}$	109	C	...
210210A	...	GRB	...	0.715	6.6 ± 0.59	0.17	$28.469^{+12.348}_{-18.3}$	4.42

Table 7. (*continued*)

GRB ID	t_p^* (days)	$\Delta m_{15,\text{bol}}$ (mag)	E_K (10^{52} erg)	M_{ej} (M_\odot)	M_{Ni} (M_\odot)	v_{ph} (km/s)	k_{avg}	s_{avg}
910423
951107C
960221
960925
961218
970228
970508
970514	...	30	5	2.6	15000 $^-$
971013
971115	20^{+4}_{-4}	7.6^{+2}_{-2}	$0.15^{+0.02}_{-0.02}$
971120	13000 $^-$
971221
980326	8^{+2}_{-2}	$0.45^{+0.15}_{-0.15}$	18000 $^-$
980425	15.16	0.8	25^{+5}_{-5}	1	1
980525
980703
980910
990712	$26.1^{+24.6}_{-15}$	$6.6^{+3.5}_{-2.9}$	$0.14^{+0.04}_{-0.04}$...	0.36 ± 0.05	0.94 ± 0.12
990902
991002
991021	$1.3^{+0.8}_{-0.5}$	$2.9^{+0.9}_{-0.7}$	$0.15^{+0.04}_{-0.03}$
991208	$38.7^{+44.6}_{-26}$	$9.7^{+6.8}_{-5.6}$	$0.96^{+0.48}_{-0.48}$...	2.11 ± 0.58	1.1 ± 0.2
000114
000418
000911	0.85 ± 0.35	1.4 ± 0.32
011121	1.7	...	$17.7^{+8.8}_{-6.4}$	$4.4^{+0.8}_{-0.8}$	$0.35^{+0.01}_{-0.01}$...	1.13 ± 0.23	0.84 ± 0.17
020405	$8.9^{+5.4}_{-3.8}$	$2.2^{+0.6}_{-0.5}$	$0.23^{+0.02}_{-0.02}$...	0.82 ± 0.14	0.62 ± 0.03
020903	$28.9^{+32.2}_{-18.9}$	$7.3^{+4.9}_{-4}$	$0.25^{+0.13}_{-0.13}$...	0.61 ± 0.19	0.98 ± 0.02
021211	28.5^{+45}_{-13}	$7.2^{+7.4}_{-6}$	$0.16^{+0.14}_{-0.14}$...	0.4 ± 0.19	0.98 ± 0.26
030329	12.75	0.7	35^{+15}_{-15}	$7.5^{+2.5}_{-2.5}$	$0.5^{+0.1}_{-0.1}$	20000 $^-$	1.28 ± 0.28	0.87 ± 0.18
030723
031203	17.33	0.62	60^{+15}_{-15}	13^{+4}_{-4}	$0.55^{+0.2}_{-0.2}$	18000 $^-$	1.65 ± 0.36	1.1 ± 0.24
040924	0.203 ± 0.202	1.371 ± 0.971
041006	$76.4^{+39.8}_{-28.7}$	$19.2^{+3.9}_{-3.6}$	$0.69^{+0.07}_{-0.07}$...	1.16 ± 0.06	1.47 ± 0.04
050416A
050525A	$18.9^{+10.7}_{-7.5}$	$4.8^{+1.1}_{-1}$	$0.24^{+0.02}_{-0.02}$...	0.69 ± 0.03	0.83 ± 0.03

Table 7 *continued on next page*

Table 7 (continued)

GRB ID	t^* (days)	$\Delta m_{15,\text{bol}}$ (mag)	E_K (10^{52} erg)	M_{ej} (M_\odot)	M_{Ni} (M_\odot)	v_{ph} (km/s)	k_{avg}
050824	5.7 $^{+9.3}_{-3.7}$	1.4 $^{+1.6}_{-0.6}$	0.26 $^{+0.17}_{-0.17}$	1.05 ± 0.42	0.52 ± 0.14
060218	10.42	0.83	1.0 $^{+0.5}_{-0.5}$	2.0 $^{+0.5}_{-0.5}$	0.20 $^{+0.10}_{-0.10}$	200000 $^{-}$	0.58 ± 0.13
060729	24.4 $^{+14.3}_{-9.9}$	6.1 $^{+1.6}_{-1.4}$	0.36 $^{+0.05}_{-0.05}$...	0.94 ± 0.1
060904B	9.9 $^{+5.1}_{-3.7}$	2.5 $^{+0.5}_{-0.5}$	0.12 $^{+0.01}_{-0.01}$...	0.42 ± 0.02
070419A	0.65 ± 0.01
071025
071112C	11.9	...	7.0 $^{+1.0}_{-1.0}$	7.0 $^{+2.0}_{-2.0}$	0.09 $^{+0.02}_{-0.02}$	300000 $^{-}$	0.6 ± 0.1
080109	19.30	...	22.7 $^{+19.1}_{-11.9}$	5.7 $^{+2.6}_{-2.2}$	0.86 $^{+0.45}_{-0.45}$...	0.75 ± 0.15
080319B	19 $^{+15}_{-15}$	2.3 $^{+1}_{-1}$	0.39 $^{+0.08}_{-0.08}$
081007A	12	...	36.5 $^{+20}_{-14.2}$	9.2 $^{+2.1}_{-1.9}$	0.37 $^{+0.03}_{-0.03}$...	0.89 ± 0.1
090618	13.5 $^{+0.4}_{-0.4}$	4.7 $^{+0.1}_{-0.1}$	0.33 $^{+0.01}_{-0.01}$	17000 $^{+2500}_{-2500}$	0.85 ± 0.11
091127	15	0.5	15.4 $^{+1.4}_{-1.4}$	2.5 $^{+0.2}_{-0.2}$	0.12 $^{+0.02}_{-0.02}$	35000 $^{-}$	0.98 ± 0.2
100316D	8.76	0.89	0.88 ± 0.01
100418A	10 $^{+6}_{-6}$	1.3 $^{+0.5}_{-0.5}$	0.43 $^{+0.03}_{-0.03}$...	0.53 ± 0.11
101219B	11.8	0.99	32 $^{+16}_{-16}$	8.1 $^{+1.5}_{-1.5}$	0.41 $^{+0.03}_{-0.03}$	19934 $^{-}$	0.76 ± 0.1
101225A	55 $^{+35}_{-35}$	4.0 $^{+1.0}_{-1.0}$	1.0 $^{+0.1}_{-0.1}$	21000 $^{-}$	0.96 ± 0.05
111220A	14.80	0.78	1.02 ± 0.03
111221A	1.11 ± 0.22
111228A	22.7	1.08 ± 0.11
120422A	14.45	0.62	25.5 $^{+2.1}_{-2.1}$	6.1 $^{+0.5}_{-0.5}$	0.57 $^{+0.07}_{-0.07}$	20500 $^{-}$	1.81 ± 0.19
120714B	13.6	0.18	42000 $^{+5500}_{-5500}$	0.86 ± 0.04
120729A	1.02 ± 0.26
130215A	1
130427A	13	0.56 $^{+0.21}_{-0.18}$...	0.675 ± 0.075
130702A	12.94	0.85	8.2 $^{+0.4}_{-0.4}$	3.1 $^{+0.1}_{-0.1}$	0.37 $^{+0.01}_{-0.01}$	21300 $^{-}$	0.77 ± 0.03
130831A	11.9	...	18.7 $^{+9}_{-9}$	4.7 $^{+0.8}_{-0.8}$	0.3 $^{+0.07}_{-0.07}$	30300 $^{+6000}_{-6000}$	0.98 ± 0.07
140206A	0.82 ± 0.19
140606B	19 $^{+11}_{-11}$	4.8 $^{+1.9}_{-1.9}$	0.42 $^{+0.17}_{-0.17}$	19800 $^{-}$	0.93 ± 0.19
150818A	1.04 ± 0.24
161219B	51 $^{+8}_{-8}$	5.8 $^{+0.3}_{-0.3}$	0.22 $^{+0.08}_{-0.08}$	29700 $^{+1500}_{-1500}$	0.81 ± 0.13
161228B	16.47	...	4	2	0.64 $^{+0.065}_{-0.059}$	16900 $^{-}$...
171010A	8.1 $^{+2.5}_{-2.5}$	4.1 $^{+0.7}_{-0.7}$	0.33 $^{+0.02}_{-0.02}$	14000 $^{+1000}_{-1000}$	0.78 ± 0.05
171205A	4.9 $^{+0.9}_{-0.9}$	0.18 $^{+0.01}_{-0.01}$	22000 $^{-}$...	0.82 ± 0.19
180720B
180728A
190114C	13.5 $^{+5.08}_{-5.08}$	5.67 $^{+0.72}_{-0.72}$	0.5 $^{+0.1}_{-0.1}$
190829A
200826A	1.45 ± 0.27	1
210210A

Table 7. (continued)

GRB ID	SN ID	$\log_{10} T_{\text{a,opt}}^*$	$\log_{10} L_{\text{a,opt}}$	$\log_{10} T_{\text{e,X}}^*$	$\log_{10} L_{\text{a,X}}$	θ_{jet}	T_{jet}	Sources
		(s)	(ergs $^{-1}$)	(s)	(ergs $^{-1}$)	($^{\circ}$)	(days)	
910423	1991aa	(3), (53)
951107C	1995bc	(32)
960221	1996N	(54)
960925	1996at	(32), (54)
961218	1997B	(1),(17)
970228	
970508	16.79 \pm 3.30	25.00 \pm 5.00	(4), (7), (8), (54)	
970514	1997cy	(2), (18), (33)
971013	1997dq	(33), (54)
971115	1997ef	(33),
971120	1997ei	(54)
971221	1997ey	(4), (30)
980326	> 5.08	0.4	(1), (5), (17)	
980425	1998bw	11.00 \pm 3.00	(13)
980525	1998ce	(63)
980703	11.00 \pm 0.80	3.40 \pm 0.50	(6), (17), (49)	
980910	1999E	(4), (30), (33), (34), (35)
990712	> 23.55	11.57 \pm 0.20	(1), (7), (8)	
990902	1999dp	(4)
991002	1999eb	(4), (33), (36), (60), (61)
991021	1999ex	(37), (55)
991208	< 4.53	2.1	(1), (7)	
000114	2000C	(4)
000418	11.35	...	(6), (7), (17)	
000911	< 4.4	(1)
011121	2001ke	4.49 \pm 0.16	...	(1), (17), (30), (38)	
020405	6.40 \pm 1.05	1.67 \pm 0.52	(1), (17), (50)	
020903	(1), (17)
021211	2002lt	4.82 \pm 0.68	...	(1), (8), (17)	
030329	2003lh	5.43 \pm 0.05	44.11 \pm 0.09	...	3.80 \pm 0.05	0.47 \pm 0.05	(1), (8), (10), (17)	
030723	(9), (39), (57), (58), (59)
031203	2003lw	9.00 \pm 2.00	...	(1), (6), (57)	
040924	...	3.23 \pm 0.04	45.26 \pm 0.13	...	> 6.9	...	(1), (8), (17)	
041006	...	3.84 \pm 0.03	44.76 \pm 0.07	...	2.90 \pm 0.40	...	(1), (8), (17)	
050416A	...	3.93 \pm 0.06	43.70 \pm 0.08	2.78 \pm 0.07	46.69 \pm 0.05	...	(1)	
050525A	2005nc	3.69 \pm 0.04	45.51 \pm 0.04	...	2.12 \pm 0.46	0.16 \pm 0.09	(1), (30)	

Table 7 continued on next page

Table 7 (*continued*)

NOTE—Sources. (1):Cano et al. (2014), (2):Cano et al. (2014), (3):Schmidt (2005), (4):Bosnjak et al. (2006), (5):Qin & Chen (2013), (6):Minaev & Pozanenko (2019), (7):Frail et al. (2001), (8) Ghirlanda et al. (2004) , (9):Butler et al. (2005), (10):Perley et al. (2010), (11):Klotz et al. (2008), (12):Starling et al. (2010), (13):Derei et al. (2017), (14):von Kienlin et al. (2020), (15):Bartoli et al. (2017), (16):Rhodes et al. (2021), (17):Demianski et al. (2017), (18):Turatto et al. (2000), (19):Li (2008b), (20):Götz et al. (2014), (21):Corsi et al. (2017), (22):Dado et al. (2002), (23):Zhang et al. (2019), (24):Klose et al. (2021), (25):Melandri et al. (2019), (26):Hu et al. (2021), (27):Izzo et al. (2019), (28):Toffano et al. (2021), (29):Kann et al. (2019) , (30):Lü et al. (2018) ,(31) : Rossi et al. (2021), (32) : BATSEGRB,(33) : Nomoto et al. (2000),(34) : Germany et al. (2000),(35) : Rigon et al. (2003),(36) : Li et al. (2002), ,(37):Lyman et al. (2016),(38):Garnavich et al. (2003), (39):HETE, (40) : Soderberg et al. (2008),(41) : Ruffini et al. (2021),(42) : Bianco et al. (2014), (43) : Prentice et al. (2016),(44) : Mazzali (2011),(45): Berger et al. (2011), (46):OSC , (47): Wang et al. (2019), (48) : Amati et al. (2002), (49): Kong et al. (2009), (50):Price et al. (2003), (51):Liang et al. (2008), (52):Zhao et al. (2020), (53):Hudec et al. (1999) , (54):Wang & Wheeler (1998), (55):Stritzinger et al. (2002), (56):Berger et al. (2011), (57):Fynbo et al. (2004), (58):Pian et al. (2005), (59):Tominaga et al. (2004), (60):Madjaz et al. (1999), (61):Terlevich & al (1999), (62):https://gen.gsfc.nasa.gov/gen3/7627.gen3, (63):IAUC 6955, (64):NASA/GSFC LHEA GCN Bacodine, (65):Lin et al. (2020), (66):Cano et al. (2017b), (67):Ashall et al. (2019). Other information come from The Open Supernova Catalog <https://sne.space> (Guillochon et al. 2017) and the Transient Name Server <https://www.wis-tns.org/>.